Glycoconj J (2015) 32:49–67
DOI 10.1007/s10719-014-9570-6

ORIGINAL ARTICLE

Molecular modeling of methyl-α-Neu5Ac analogues docked against cholera toxin - a molecular dynamics study

J. Jino Blessy · D. Jeya Sundara Sharmila

Received: 11 August 2014 / Revised: 26 November 2014 / Accepted: 27 November 2014 / Published online: 13 February 2015

Abstract Molecular modeling of synthetic methyl-α-Neu5Ac analogues modified in C-9 position was investigated by molecular docking and molecular dynamics (MD) simulation methods. Methyl-α-Neu5Ac analogues were docked against cholera toxin (CT) B subunit protein and MD simulations were carried out for three Methyl-α-Neu5Ac analogue-CT complexes (30, 10 and 10 ns) to estimate the binding activity of cholera toxin-Methyl-α-Neu5Ac analogues using OPLS_2005 force field. In this study, direct and water mediated hydrogen bonds play a vital role that exist between the methyl-α-9-*N*-benzoyl-amino-9-deoxy-Neu5Ac (BENZ)-cholera toxin active site residues. The Energy plot, RMSD and RMSF explain that the simulation was stable throughout the simulation run. Transition of phi, psi and omega angle for the complex was calculated. Molecular docking studies could be able to identify the binding mode of methyl-α-Neu5Ac analogues in the binding site of cholera toxin B subunit protein. MD simulation for Methyl-α-9-*N*-benzoyl-amino-9-deoxy-Neu5Ac (BENZ), Methyl-α-9-*N*-acetyl-9-deoxy-9-amino-Neu5Ac and Methyl-α-9-*N*-biphenyl-4-acetyl-deoxy-amino-Neu5Ac complex with CT B subunit protein was carried out, which explains the stable nature of interaction. These methyl-α-Neu5Ac analogues that have computationally acceptable pharmacological properties may be used as novel candidates for drug design for cholera disease.

Keywords Methyl-α-Neu5Ac analogues · Cholera toxin · Molecular dynamics

D. J. S. Sharmila (✉)
Department of Nano Science and Technology, Tamil Nadu Agricultural University, Coimbatore 641003, Tamil Nadu, India
e-mail: djssharmila@gmail.com

J. J. Blessy
Department of Bioinformatics, Karunya University, Karunya Nagar, Coimbatore 641114, Tamil Nadu, India

Introduction

The family of sialic acid (Neu5Ac or NeuNAc) contains more than 30 derivatives of naturally occurring neuraminic acid [1]. Among them *N*-Acetylneuraminic acid (Neu5Ac) is the most predominant sialic acid found in the cell surface of glycoproteins and glycolipids that plays a vital role in the carbohydrate–protein recognizing events such as cell adhesion, leukocytes extravasation and bacterial & viral infections. Sialic acid has the ability to inhibit target proteins like sialoadhesins, selectins, and hemagglutinin (influenza), it might show strong antiviral or antibacterial and anti-inflammatory effects [2, 3]. Sialic acid exposes to the cellular environment and involves in intrinsic & extrinsic communication and in defense mechanism. It also protects epithelial tissues from harmful substances and infectious agents [4, 5]. Sialic acid acts as a biological mask for cellular receptors. The TrKA tyrosine kinase receptors, recognized as signaling receptors for neurotrophin growth factor was activated by the removal of 2,3-linked Sialic acid from the Gal residues [6]. Sialic acid acts as ligands for proteins or receptors of vertebrate cells, viruses, bacteria, lectins, toxins, protozoa, mycoplasma and antibodies [7]. In Methyl-α-Neu5Ac analogues, the hydroxyl group at C-9 position of Neu5Ac glycerol side chain was substituted by different functional group which was synthesized based on Mitsunobu reaction [8].

Sialic acid binds to the toxins secreted by *Vibrio*, *Clostridium* species, *Escherichia coli* and *Bordetella pertussis* [9]. Cholera toxin (CT) is made up of AB_5 hexamer with a single A subunit and five B subunits. Bacterial enterotoxins such as *Escherichia coli* heat-labile enterotoxin (LT), pertussis toxin, diphtheria toxin, shigella toxin, and *Pseudomonas aeruginosa* exotoxin A, are structurally and functionally related to cholera toxin. The biological functions of each of these toxins are separated into distinct domains. Cell recognition and binding of CT and LT are carried out by the B-

pentamer. After the binding of holotoxin to the cell membrane, the A subunit is directed into the target cell. But, till now this mechanism is not known in detail. The cell surface receptor of CT and LT is the pentasaccharide which is linked to the ganglioside (GM1) [10]. Neu5Ac acts as a significant molecule for cholera toxin binding and drugs designed to inhibit Neu5Ac binding could be able to prevent cholera infection [11–13].

In the current study, the C-9 position of methyl-α-Neu5Ac analogues were modified and modeled to analyze the binding mode of methyl-α-Neu5Ac into the active site of cholera toxin protein. Even though sufficient numbers of inhibitors were already reported [14] for cholera toxin including recent multivalent inhibitor reported by Branson *et al.*, 2014 [15] the present methyl-α-Neu5Ac analogues were not yet studied as monovalent/multivalent inhibitors against cholera toxin. Hence, the present design and dynamics studies of methyl-α-Neu5Ac analogues into the binding pocket of cholera toxin is an attempt to disclose additional information that might be helpful for further design of potential multivalent inhibitors against cholera. The 3D structure of cholera toxin B subunit protein (PDB ID: 3CHB) [16] was downloaded from protein data bank (PDB). Molecular modeling of methyl-α-Neu5Ac analogues were accomplished using the chemical drawing software chemsketch. Molecular docking is a technique to predict the binding orientation of two molecules when bound to one another to form stable complex [17]. Docking of methyl-α-Neu5Ac analogues against cholera toxin protein was performed using Glide v5.7 software in Schrödinger suite [18]. In the C-9 position of glycerol side chain of each methyl-α-Neu5Ac analogue, the terminal hydroxyl group (OH) was substituted with different functional groups. Seven methyl-α-Neu5Ac analogues were modeled and docked as follows: methyl-α-Neu5Ac, methyl-α-9-*N*-benzoyl-amino-9-deoxy-Neu5Ac (BENZ), methyl-α-9-*N*--(naphthyl-2-carbonyl)-amino-9-deoxy-Neu5Ac (NAP), methyl-α-9-*N*-(biphenyl-4-carbonyl)-amino-9-deoxy-Neu5Ac (BIP), methyl-α-9-*N*-biphenyl-4-acetyl-deoxy-amino-Neu5Ac, methyl-α-9-*N*-acetyl-9-deoxy-9-amino-Neu5Ac and methyl-α-9-deoxy-Neu5Ac. Protein-carbohydrate binding was reported for multivalent ligands designed for improved inhibition for carbohydrate binding sites of bacterial toxin such as CT, LT and shiga toxin [14]. And also this study was carried out for the ADME prediction to identify the pharmacokinetic properties of Methyl-α-Neu5Ac analogues. Molecular dynamics simulation is a computational method to calculate the physical movement and time- dependent behavior of atoms and molecules in molecular system [19]. MD simulation was done for CT- Methyl-α-9-*N*-benzoyl-amino-9-deoxy-Neu5Ac (BENZ) complex, CT-Methyl-α-9-*N*-acetyl-9-deoxy-9-amino-Neu5Ac complex and CT-Methyl-α-9-*N*-biphenyl-4-acetyl-deoxy-amino-Neu5Ac complex to identify the enhanced binding mode and stability in aqueous environment. MD simulation was done using the software Desmond v3.0 [20].

Materials and methods

Molecular modeling of methyl-α-Neu5Ac analogues

Modifications done in C-9 positions of each methyl-α-Neu5Ac analogues were shown in (Table 1). The methyl-α-Neu5Ac analogues were modeled based on the literature [8]. Seven methyl-α-Neu5Ac analogues were modeled and drawn using chemical drawing software ACD/chemsketch in which 2D structure was converted into 3D representation. Using ACD/chemsketch, the user can sketch the chemical structures of organics, organometallics and polymer structures. And also using this, we can calculate other molecular properties like molecular weight, density, molar refractivity *etc.* (http://www.acdlabs.com/resources/freeware/chemsketch). The initial conformation of C-9 substituted glycerol side chain of methyl-α-Neu5Ac analogues are defined as follow: χ_1=0 when C5-C6 cis to C7-C8; χ_2=0 when C6-C7 cis to C8-C9.

Molecular docking of methyl-α-Neu5Ac analogues against cholera toxin

The three dimensional structure of cholera toxin protein (PDB ID: 3CHB) [16] was downloaded from protein data bank (PDB). The active site residues of cholera toxin protein structure were analyzed using PDBsum pictorial database. Tertiary structure of cholera toxin protein and methyl-α-Neu5Ac analogues were imported to Maestro v9.0 environment [21] to investigate molecular docking binding affinity of methyl-α-Neu5Ac analogues towards cholera toxin. Each atom of proteins and ligands must be fixed before molecular docking for accurate prediction of binding affinity and interactions. The cholera toxin protein structure was preprocessed using protein preparation wizard in maestro v9.2. Hydrogen atoms were added to cholera toxin protein which subsequently was minimized with the OPLS_2005 force field [22] and the impact molecular mechanics engine sets the maximum RMSD value of 0.03 Å. Impref (Impact Refinement module) minimization was preformed which was the final step in protein preparation process which is used to refine the protein structure. The chemical compounds were prepared using LigPrep tool from Schrödinger suite which is used to convert 2D to 3D structure. From each single input, ligPrep produce a single, low energy, three dimensional structure with correct chiralities with different stereo chemistries, tautomers, ionization states and ring conformation. The compounds with poor pharmacological properties were eliminated based on molecular weight and functional group present in it [23, 24]. Glide (grid-based ligand docking with energetics) is the docking methodology

Table 1 Methyl-α-Neu5Ac analogues withC-1/C-2/ and C-9 Modification

Sl. No	Methyl-α-Neu5Ac derivatives	Substituent		
	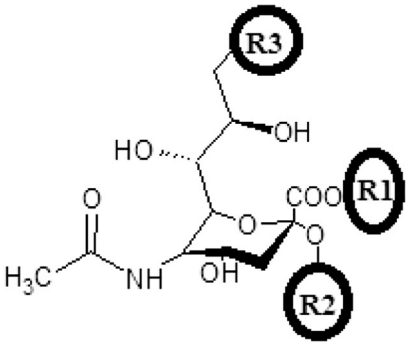	R1	R2	R3
1	Methyl-α-Neu5Ac	H	CH_3	OH
2	Methyl-α-9-*N*-benzoyl-amino-9-deoxy-Neu5Ac (BENZ)	H	CH_3	C_6H_5CONH
3	Methyl-α-9-*N*-(naphthyl-2-carbonyl)-amino-9-deoxy-Neu5Ac (NAP)	H	CH_3	$C_{10}H_7CONH$
4	Methyl-α-9-*N*-(biphenyl-4-carbonyl)-amino-9-deoxy-Neu5Ac (BIP)	H	CH_3	$C_{12}H_9CONH$
5	Methyl-α-9-*N*-biphenyl-4-acetyl-deoxy-amino-Neu5Ac	H	CH_3	$C_{13}H_{10}CONH$
6	Methyl-α-9-*N*-acetyl-9-deoxy-9-amino-Neu5Ac	H	CH_3	CH_3CONH
7	Methyl-α-9-deoxy-Neu5Ac	H	CH_3	H

which was performed for a thorough search of positional, orientational and conformational space of the ligands. To locate the ligands into the active site of receptor, glide uses series of hierarchical filters, such as, ligand conformation, site-point search, diameter test, subset test, greedy score, refinement, grid minimization (Monte carlo), final scoring (glide score), top hits [25]. A receptor grid [25] 20×20×20 Å was generated around the active site residues of cholera toxin protein using Glide v5.7 [18]. Molecular docking calculation was performed using Glide v5.7. The prepared, optimized and minimized ligands were flexibly docked in the receptor grid box using Monte Carlo based simulation algorithm (MCSA). Two subsequent docking methods, glide standard precision (SP) and extra precision (XP) were used. SP docking is default which is used to screen large number of ligands of unknown quality. XP docking is more powerful which has perceptive procedure and its run time is longer than SP. During XP docking, 10,000 poses were generated for each ligand which was highly accurate and report the best docked structure based on the energy term Emodel. The best pose of each structure was further ranked based on XPGscore. The least XPGscore for a ligand indicates better binding affinity towards active site residues.

ADME prediction

Absorption, Distribution, Metabolism, and Excretion (ADME) properties were predicted using the program, QikProp. It is quick, accurate and easy to predict the ADME activity of organic structures, which has physically and pharmaceutically relevant properties. It also compares the chemical properties with 95 % of known drugs [26, 27]. It was used to predict the Pharmaceutical properties for the prepared ligands which was assessed through Lipinski's rule of five [28]. In QikProp, total 44 properties can be predicted for the chemical compounds. The properties analyzed for the analogues were hydrogen bond donors, hydrogen bond acceptors, molecular weight, water partition coefficient (QPlogPo/w), Predicted brain/blood partition coefficient (QPlogBB), Lipinski's rule of five (LROF) and predicted gut-blood barrier & cell permeability (QPPCaco) for the estimation of absorption and distribution of drug molecules within the body.

Molecular dynamic simulations

Molecular dynamic (MD) simulation was performed for the docking complex of CT- methyl-α-9-*N*-benzoyl-amino-9-deoxy-Neu5Ac (BENZ) for 30 ns, CT-Methyl-α-9-*N*-acetyl-9-deoxy-9-amino-Neu5Ac for 10 ns and CT-Methyl-α-9-*N*-biphenyl-4-acetyl-deoxy-amino-Neu5Ac for 10 ns to evaluate the stability, conformational change and to get insights of the natural dynamic at different timescales. Simulation was performed using Desmond v3.0 [20] which was implemented in Schrödinger package for 30, 10 and 10 ns simulation time. Desmond is a new explicit solvent MD simulation program which was developed by D.E. Shaw research laboratory. It has the features of highly scalable parallel execution, periodic boundary conditions, pressure coupling like isotropic, semi-isotropic and anisotropic and ensembles like NPT, NVT,

NVE, NPAT, NPγT *etc.* [20]. The MD simulation for the cholera toxin- methyl-α-Neu5Ac analogues complex was performed by applying OPLS_2005 force field. The system was embedded with TIP3P water model [29] and neutralized by replacing solvent molecules with counter ions Na^+ and Cl^-. The full system of CT- methyl-α-9-*N*-benzoyl-amino-9-deoxy-Neu5Ac (BENZ) complex consists of approximately 19,470 atoms, CT-Methyl-α-9-*N*-acetyl-9-deoxy-9-amino-Neu5Ac complex composed of 19,517 atoms and CT-Methyl-α-9-*N*-biphenyl-4-acetyl-deoxy-amino-Neu5Ac complex contains 19,627 atoms. This was simulated through a multistep protocol, devised in Desmond. Non hydrogen solute atoms were restrained in NPT ensemble (constant number of atom (N), pressure (P) and temperature (T)) and the system is equilibrated for the simulation time of 24 picoseconds (ps) at the temperature of 300 K. During MD simulation, the system was studied for the simulation time of 30,000, 10,000 and 10,000 ps. The particle-mesh Ewald (PME) algorithm was used to calculate the Long-Range electrostatic interaction [30, 31]. SHAKE algorithm was applied to all the hydrogen atoms [32] and van der Waals was set to a cutoff value of 9 Å. Trajectories structural data frames were collected for every 4.8 ps during the simulation run. Energy fluctuations, RMSD for backbone and heavy atom of the cholera toxin- methyl-α-Neu5Ac analogues complex was analyzed in the trajectory data. RMSF for backbone and side chain of each residue for cholera toxin protein were monitored for consistency. The inter molecular hydrogen bonding interaction of cholera toxin- methyl-α-Neu5Ac analogues complex was assessed for stability. The backbone torsion angles phi ( ), psi (ψ) and omega (ω) for the active site amino acid residues and χ_1, χ_2 torsions for three methyl-α-Neu5Ac analogues at C-5, C-6, C-7, C-8 and C-9 position were calculated.

Result and discussion

Retrieval of cholera toxin B subunit (3CHB)

Cholera toxin B subunit protein (PDB ID: 3CHB) in complex with GAL-NGA-GAL-GLC-SIA (GM1) of *Vibrio cholera* was retrieved from protein data bank (PDB). The 3CHB protein consists of 103 amino acid residues in each B subunits. The active site residues were defined using PDBSum database. The active site residues of cholera toxin, GLU:11, TYR:12, HIS:13, GLY:33, LYS:34, GLU:51, GLN:56, HIE:57, ILE:58, GLN:61, TRP:88, ASN:90 and LYS:91 were considered as important binding site residues. These residues were involved in intermolecular hydrogen bond with GAL-NGA-GAL-GLC-SIA.

Molecular docking

Methyl-α-Neu5Ac analogues were bound to cholera toxin protein with inter molecular hydrogen bonding in addition to hydrophobic and van der Waals force.

CT- methyl-α-9-*N*-benzoyl-amino-9-deoxy-Neu5Ac (BENZ) complex

The analogue Methyl-α-9-*N*-benzoyl-amino-9-deoxy-Neu5Ac (BENZ) has the lowest XPG score of −7.55 and glide energy of −41.48 kcal/mol. The analogue was bound to cholera toxin protein with three hydrogen bonds as follows: the oxygen atom (O) interacted with atom HE21 of polar side chain residue GLN:61 with a intermolecular hydrogen bond distance of 2.012 Å, the hydrogen atom 49 (H) [OH of C-8] interacted with oxygen atom (O) of non-polar residue ALA:97 with a distance of 1.860 Å, the hydrogen atom 35 (H) [OH of C-4] interacted with oxygen atom (O) of non-polar residue ILE:99 with a distance of 1.712 Å (Fig. 1).

CT- Methyl-α-Neu5Ac complex

The analogue Methyl-α-Neu5Ac had an XPG score of −7.42 and glide energy of −37.58 kcal/mol. The analogue was bound to cholera toxin protein with five hydrogen bonds. They were, the H-bond formed by the hydrogen atom 41 (H) [OH of C-8] with oxygen atom (O) of basic polar side chain residue HIS:13 with a distance of 2.012 Å, the H-bond formed by the hydrogen atom 39 (H) [OH of C-9] with oxygen (O) of basic polar side chain residue HIS:13 with a distance of 1.924 Å, the H-bond formed by the oxygen atom (O) with HE1 of non-polar side chain residue TRP:88 with a distance of 2.010 Å, the H-bond formed by the oxygen atom (O) with HD22 of polar side chain residue ASN:90 with a distance of 1.757 Å & the H-bond formed by the oxygen atom 41 (O) with HZ1 of basic polar side chain residue LYS:91 with a distance of 1.874 Å.

CT- Methyl-α-9-*N*-acetyl-9-deoxy-9-amino-Neu5Ac complex

The analogue Methyl-α-9-*N*-acetyl-9-deoxy-9-amino-Neu5Ac had an XPG score of −7.13 and glide energy of −41.37 kcal/mol. The analogue was bound to cholera toxin protein with five hydrogen bonds. They are, the hydrogen atom 42 (H) [NH of C-9 substituent] formed a H-bond with oxygen atom (O) of basic polar side chain residue HIS:13 with a distance of 2.066 Å, the hydrogen atom 44 (H) [OH of C-8] formed a H-bond with oxygen atom (O) of basic polar side chain residue HIS:13 with a distance of 1.793 Å, the oxygen atom (O) formed a H-bond with HE1 of nonpolar side chain residue TRP:88 with a distance of 2.201 Å, the oxygen atom (O) formed a H-bond with HZ1 of basic polar side chain

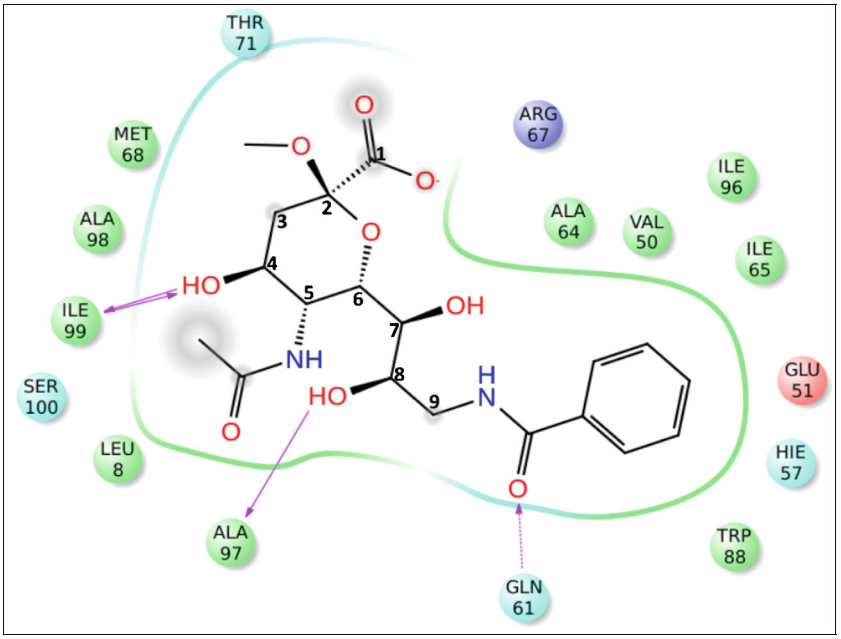

Fig. 1 Methyl-α-9-*N*-benzoyl-amino-9-deoxy-Neu5Ac (BENZ) at the binding site of Cholera toxin B subunit protein (Note: ••••••• H-bond (side chain), ——— H-bond (backbone))

residue LYS:91 with a distance of 1.781 Å & the oxygen atom (O) formed a H-bond with HD22 of polar side chain residue ASN:90 with a distance of 1.884 Å.

CT- Methyl-α-9-*N*-biphenyl-4-acetyl-deoxy-amino-Neu5Ac complex

The analogue Methyl-α-9-*N*-biphenyl-4-acetyl-deoxy-amino-Neu5Ac had an XPG score of −6.74 and glide energy of −48.75 kcal/mol. The analogue was bound to cholera toxin protein with five hydrogen bonds. They were, the H-bond formed by the hydrogen atom 56 (H) [OH of C-8] with oxygen atom (O) of basic polar side chain residue HIS:13 with a distance of 2.188 Å, the H-bond formed by the oxygen atom (O) with H of basic polar side chain residue HIS:13 with a distance of 2.114 Å, the H-bond formed by the oxygen atom (O) with HD22 of polar side chain residue ASN:90 with a distance of 2.162 Å, the H-bond formed by the oxygen atom 68 (O) with HZ1 of basic polar side residue LYS:91 with a distance of 1.797 Å & the H-bond formed by the oxygen atom (O) with HE22 of polar side chain residue GLN:61 with a distance of 2.201 Å.

CT- Methyl-α-9-deoxy-Neu5Ac complex

The analogue Methyl-α-9-deoxy-Neu5Ac had an XPG score of −6.66 and glide energy of −37.96 kcal/mol. The analogue was bound to cholera toxin protein with five hydrogen bonds. They were, the H-bond formed by the hydrogen atom 40 (H) [OH of C-8] interacted with oxygen atom (O) of basic polar side chain residue HIS:13 with a distance of 1.913 Å, the H-bond formed by the oxygen atom (O) interacted with HE1 of nonpolar side chain residue TRP:88 with a distance of 2.050 Å, the H-bond formed by the hydrogen atom 27 (H) [OH of C-4] interacted with oxygen atom (O) of polar side chain residue GLN:56 with a distance of 2.002 Å, the H-bond formed by the oxygen atom (O) interacted with HD22 of polar side chain residue ASN:90 with a distance of 1.800 Å & the H-bond formed by the oxygen atom 41 (O) interacted with HZ1 of basic polar side chain residue LYS:91 with a distance of 1.848 Å.

CT- Methyl-α-9-*N*-(biphenyl-4-carbonyl) -amino-9-deoxy-Neu5Ac (BIP) complex

The analogue Methyl-α-9-*N*-(biphenyl-4-carbonyl)-amino-9-deoxy-Neu5Ac (BIP) had an XPG score of −6.55 and glide energy of −39.72 kcal/mol. The analogue was bound to cholera toxin protein with four hydrogen bonds. They were, the H-bond formed by the interaction of the hydrogen atom 55 (H) [OH of C-8] with oxygen atom (O) of basic polar side chain residue HIS:13 with a distance of 1.893 Å, the H-bond formed by the interaction of the hydrogen atom 53 (H) [NH of C-9 substituent] with oxygen atom (O) of basic polar side chain residue HIS:13 with a distance of 2.390 Å, the H-bond formed by the interaction of the oxygen (O) with HD22 of polar side chain residue ASN:90 with a distance of 1.736 Å & the H-bond formed by the interaction of the oxygen 65 (O) with HZ1 of basic polar side chain residue LYS:91 with a distance of 1.985 Å.

CT- methyl-α-9-*N*-(naphthyl-2-carbonyl) -amino-9-deoxy-Neu5Ac (NAP) complex

The analogue Methyl-α-9-*N*-(naphthyl-2-carbonyl)-amino-9-deoxy-Neu5Ac (NAP) had an XPG score of −6.52 and glide

energy of −31.40 kcal/mol. The analogue was bound to cholera toxin protein with four hydrogen bonds. They were, the H-bond formed by the interaction of the oxygen 61 (O) with HD22 of polar side chain residue ASN:90 with a distance of 1.856 Å, the H-bond formed by the interaction of the hydrogen atom 52 (H) [OH of C-7] formed H-bond with OE1 of acidic polar chain residue GLU:51 with a distance of 1.918 Å, the H-bond formed by the interaction of the oxygen atom (O) with HE22 of basic polar side chain residue GLN:61 with a distance of 2.400 Å & the H-bond formed by the interaction of the hydrogen atom 43 (H) [NH of C-5] with (O) of basic polar side chain residue GLN:56 with a distance of 2.071 Å. As reported earlier NMR titrations explain the importance of sialic acid-Siglec5 binding [33]. The complete molecular docking profile is shown in Table 2. The earlier protein-carbohydrate report explains that methyl-α-Neu5Ac analogues show better binding affinity towards the binding assays of Siglecs [8].

Pharmacology (ADME) prediction

Lipinski rule of five was used to evaluate the drug likeness or pharmacological activity of the chemical compounds which could be an orally active drug in human beings [34, 35]. Lipinski rule of five predicted for the docked analogues are shown in Table 3. The above observation has revealed that the Methyl-α-Neu5Ac analogues are pharmacological active compounds. H-bond donors, H-bond acceptors, Molecular weight, LROF (Lipinski rule of five), QPlogPo/w, QPlog MDCK, QPlogS, QPP Caco are the properties that can be used to judge the analogues as potential drug candidates. Molecular weight of each analogue falls between the ranges of 307–500 Da. QPlogS values of the analogues are within the tolerable range of 95 % of existing drug molecule. (QPP Caco) gut-blood barrier and cell permeability of the analogues are in the acceptable range. The seven analogues have acceptable pharmacological properties (Table 3) and these analogues may be used as potential drug molecule for the cholera disease.

Molecular dynamic simulation

In the present study, the dynamic properties of cholera toxin complex with Methyl-α-9-*N*-benzoyl-amino-9-deoxy-Neu5Ac (BENZ), Methyl-α-9-*N*-acetyl-9-deoxy-9-amino-Neu5Ac and Methyl-α-9-*N*-biphenyl-4-acetyl-deoxy-amino-Neu5Ac were analyzed from trajectory data obtained from 30 10 and 10 ns MD simulation run respectively. Since the flexibility of the protein molecule was not taken into deliberation in molecular docking technique, the internal motion of the receptor-ligand complex was explained in detail using molecular dynamic simulation. In flexible condition the receptor-ligand complex was treated in the solvent. In our current study, binding mode of CT- Methyl-α-9-*N*-benzoyl-amino-9-deoxy-Neu5Ac (BENZ) complex, CT- Methyl-α-9-*N*-acetyl-9-deoxy-9-amino-Neu5Ac complex and CT-Methyl-α-9-*N*-biphenyl-4-acetyl-deoxy-amino-Neu5Ac complex were analyzed by MD simulation using software Desmond. The conformational changes which occurred after MD simulation, are more stable and was closer to the physiological condition. The binding orientation of chemical compound calculated through MD simulation shows strong interaction between the receptor-ligand molecules [36–39]. In order to check the conformational variation of CT-Methyl-α-9-N-benzoyl-amino-9-deoxy-Neu5Ac (BENZ) complex, the trajectory data was plotted for RMSD (Fig. 2a and b), RMSF (Fig. 3) and Energy (Fig. 4).

MD simulation for CT-Methyl-α-9-*N*-benzoyl-amino-9-deoxy-Neu5Ac (BENZ) complex

The RMSD (root mean square deviation) value of protein backbone and heavy atoms were taken into consideration. RMSD plot revealed that the complex was comparatively stable throughout the simulation time. The backbone atoms of RMSD graph clearly indicated the fluctuations between the ranges of 0.9–2.0 Å and the heavy atoms show fluctuations between the range of 1.3–4.0 Å during 30,000 ps. The RMSF (root mean square fluctuation) value of backbone and the side chain of each active residue of cholera toxin were analyzed. The RMSF backbone fluctuated within the limit of 0.5–3.0 Å and the side chain residue fluctuations were within the limit of 0.7–3.5 Å. Maximum backbone fluctuations were up to 3.3 Å and the maximum side chain fluctuations were up to 4.4 Å. The energy calculation under simulation quality analysis revealed that the total energy of the system was −49850.844 Kcal/mol, potential energy was −62140.633 Kcal/mol, temperature was 298.644 K and the volume was 94930.369 $Å^3$. The energy plot explains that the energy of the whole system was stable throughout the simulation in 30 ns simulation run. Even though the total energy seems to increase during the initial simulation period, it gets equilibrated after 25 ns. However, the energy component responsible for structural stability is potential energy (E_P) which is well equilibrated during the simulation (−62140.633 Kcal/mol) (Fig. 4).

The hydrogen bond interaction for Methyl-α-9-*N*-benzoyl-amino-9-deoxy-Neu5Ac (BENZ) and cholera toxin complex (Fig. 5) was monitored for 6250 frames periodically collected from trajectories. The molecular dynamic simulation trajectories reproduced intermolecular hydrogen bonding between cholera toxin- Methyl-α-9-*N*-benzoyl-amino-9-deoxy-Neu5Ac (BENZ) complex (Fig. 6, Table 4). The analysis revealed that the water molecules play a vital role in cholera toxin-Methyl-α-9-*N*-benzoyl-amino-9-deoxy-Neu5Ac (BENZ) interaction. In the majority of the trajectories, active site residues of cholera toxin were involved in hydrogen bond

Table 2 Glide docking score, Glide energy and inter molecular hydrogen bond distance of Cholera toxin- Methyl-α-Neu5Ac analogues docking complex

S.No	Analogues name	XPG score	Glide energy Kcal/mol	Ligand Atom	Protein		Inter molecular hydrogen bonding distance (Å)
					Residues	Atom	
1	Methyl-α-9-*N*-benzoyl-amino-9-deoxy-Neu5Ac (BENZ)	−7.55	−41.48	O	GLN:61	HE21	2.012
				H49	ALA:97	O	1.860
				H35	ILE:99	O	1.712
2	Methyl-α-Neu5Ac	−7.42	−37.58	H41	HIS:13	O	2.012
				H39	HIS:13	O	1.924
				O	TRP:88	HE1	2.010
				O	ASN:90	HD22	1.757
				O42	LYS:91	HZ1	1.874
3	Methyl-α-9-*N*-acetyl-9-deoxy-9-amino-Neu5Ac	−7.13	−41.37	H42	HIS:13	O	2.066
				H44	HIS:13	O	1.793
				O	TRP:88	HE1	2.201
				O48	LYS:91	HZ1	1.781
				O	ASN:90	HD22	1.884
4	Methyl-α-9-*N*-biphenyl-4-acetyl-deoxy-amino-Neu5Ac	−6.74	−48.75	H56	HIS:13	O	2.188
				O	HIS:13	H	2.114
				O	ASN:90	HD22	2.162
				O68	LYS:91	HZ1	1.797
				O	GLN:61	HE22	2.201
5	Methyl-α-9-deoxy-Neu5Ac	−6.66	−37.96	H40	HIS:13	O	1.913
				O	TRP:88	HE1	2.050
				H27	GLN:56	O	2.002
				O	ASN:90	HD22	1.800
				O41	LYS:91	HZ1	1.848
6	Methyl-α-9-*N*-(biphenyl-4-carbonyl)-amino-9-deoxy-Neu5Ac (BIP)	−6.55	−39.72	H55	HIS:13	O	1.893
				H53	HIS:13	O	2.390
				O	ASN:90	HD22	1.736
				O65	LYS:91	HZ1	1.985
7	Methyl-α-9-*N*-(naphthyl-2-carbonyl)-amino-9-deoxy-Neu5Ac (NAP)	−6.52	−31.40	O61	ASN:90	HD22	1.856
				H52	GLU:51	OE1	1.918
				O	GLN:61	HE22	2.400
				H43	GLN:56	O	2.071

Table 3 QikProp (ADME) prediction for methyl-α-Neu5Ac analogues

Sl.No	Analogue name	Molecular weight	H-bond donors	H-bond acceptors	LROF	QPlogPo/w	QPlog MDCK	QPlogS	QPP Caco
1	Methyl-α-9-*N*-benzoyl-amino-9-deoxy-Neu5Ac (BENZ)	426.42	4	8	2	−0.24	6.78	−1.93	8.36
2	Methyl-α-Neu5Ac	323.29	5	9	1	−1.83	5.02	−0.27	6.27
3	Methyl-α-9-*N*-acetyl-9-deoxy-9-amino-Neu5Ac	364.35	3	7	2	−2.06	4.85	0.10	3.13
4	Methyl-α-9-*N*-biphenyl-4-acetyl-deoxy-amino-Neu5Ac	485.547	5	9	3	0.9	11.64	−2.65	8.91
5	Methyl-α-9-deoxy-Neu5Ac	307.3	5	7	0	−0.89	21.38	−0.62	24.29
6	Methyl-α-9-*N*-(biphenyl-4-carbonyl)-amino-9-deoxy-Neu5Ac (BIP)	499.52	4	7	3	1.10	7.37	−3.30	9.32
7	Methyl-α-9-*N*-(naphthyl-2-carbonyl)-amino-9-deoxy-Neu5Ac (NAP)	476.48	5	9	2	0.54	6.78	−2.82	8.37

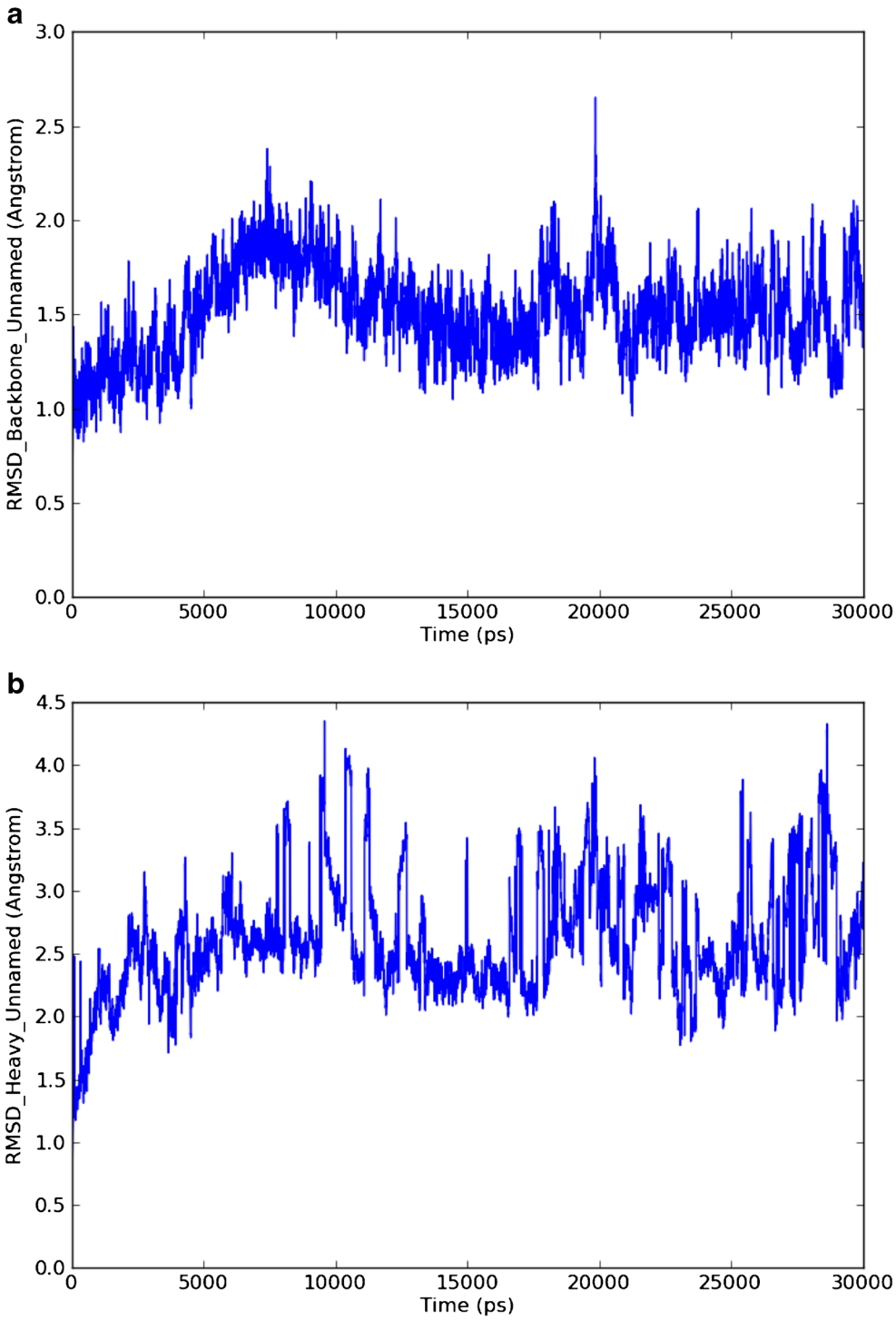

Fig. 2 Interactions of Cholera toxin- Methyl-α-9-*N*-benzoyl-amino-9-deoxy-Neu5Ac (BENZ) complex during 30 ns MD simulation run. **a** MD simulation Time vs RMSD of backbone atom cholera toxin B subunit protein. **b** RMSD of heavy atom of cholera toxin B subunit protein

through water bridges. As explained in the previous report using NMR and molecular dynamic simulation study, Carbohydrate-protein recognition of glycerol-Gal3C, lactose-Gal3c, and apo-Gal3C complex were bound into the carbohydrate binding site of Gal3C. Also, previous water dynamics documented arginine (ARG) involved hydrogen bond with carbohydrate through water bridging [40]. In the present MD trajectories, ARG:67 of CT formed two water bridged H-bonds (Table 5) and one direct H-bond with Methyl-α-9-*N*-benzoyl-amino-9-deoxy-Neu5Ac (BENZ). This result supports the earlier work on interaction of *N*-acetylglucosamine with ARG (R239) [41]. The atom 957 (O) of Methyl-α-9-N-benzoyl-amino-9-deoxy-Neu5Ac (BENZ) formed H-bond with atom (H) HH of TYR:12 with a H-bond distance of 2.210 Å, atom 48 (H) [OH of C-7] of Methyl-α-9-*N*-benzoyl-amino-9-deoxy-Neu5Ac (BENZ) formed H-bond with

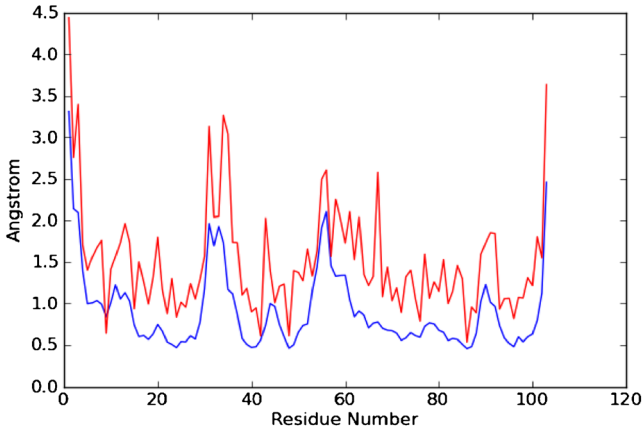

Fig. 3 RMSF of Cholera toxin- Methyl-α-9-*N*-benzoyl-amino-9-deoxy-Neu5Ac (BENZ) complex during 30 ns simulation run. Red colour indicates side chain and blue colour indicated backbone

atom (O) of ALA:64 with a distance of 2.374 Å, atom 49 (H) [NH of C-9 substituent] of Methyl-α-9-*N*-benzoyl-amino-9-deoxy-Neu5Ac (BENZ) formed H-bond with atom 828 (O) of ALA:97 with a distance of 2.104 Å, atom 35 (H) [OH of C-4] of Methyl-α-9-*N*-benzoyl-amino-9-deoxy-Neu5Ac (BENZ) formed H-bond with atom (O) of ILE:99 with a distance of 1.962 Å, atom 7 (O) of Methyl-α-9-*N*-benzoyl-amino-9-deoxy-Neu5Ac (BENZ) formed H-bond with atom 1655 (H) of ILE:99 with a distance 1.938 Å and atom 55 (O) of Methyl-α-9-*N*-benzoyl-amino-9-deoxy-Neu5Ac (BENZ) formed H-bond with atom 1387 (HH12) of ARG:67 with a distance of 1.815 Å. Including the water bridged hydrogen bonds (Table 5), totally eight hydrogen bonds were formed between cholera toxin- Methyl-α-9-*N*-benzoyl-amino-9-deoxy-Neu5Ac (BENZ) complex. The above analysis was shown in Table 4. The present docking and dynamics simulation suggest the enhanced binding of Methyl-α-9-*N*-benzoyl-amino-9-deoxy-Neu5Ac (BENZ) with cholera toxin due to the presence of aromatic ring at the C-9 modification. There is an additional π-π stacking observed between the aromatic ring at C-9 position of Methyl-α-9-*N*-benzoyl-amino-9-deoxy-Neu5Ac (BENZ) with active site residue HIS:57 (Fig. 6). Similar binding enhancement was reported by [8] for Methyl-α-9-*N*-benzoyl-amino-9-deoxy-Neu5Ac (BENZ) - sialoadhesin binding.

From the above observation of cholera toxin-Methyl-α-9-*N*-benzoyl-amino-9-deoxy-Neu5Ac (BENZ) complex, the active site residues ARG:67, ILE:99, ALA:97 and TYR:12 (Fig. 7a & b and 8a & b) were actively involved in intermolecular hydrogen bonding during 30,000 ps simulation run. There are three different types of backbone dihedral angle. They are phi ( ) angle backbone atom C-N-Cα-C, psi (ψ) angle backbone atom N-Cα-C-N and omega (ω) angle backbone atom Cα-C-N-Cα respectively. In protein backbone due to the rigid peptide bonds, phi ( ) and psi (ψ) angle decide the geometry of the backbone without considering the omega (ω) angle which would always be fixed in 180° [42]. In our current study, torsion angle were predicted for the cholera toxin active site residues ARG:67, ILE:99, ALA:97 and TYR:12. The phi ( ) torsion angle of ARG:67 shows a transition between the range of −80° to −50°, for psi (ψ) angle transition between the range of −50° to −10° and

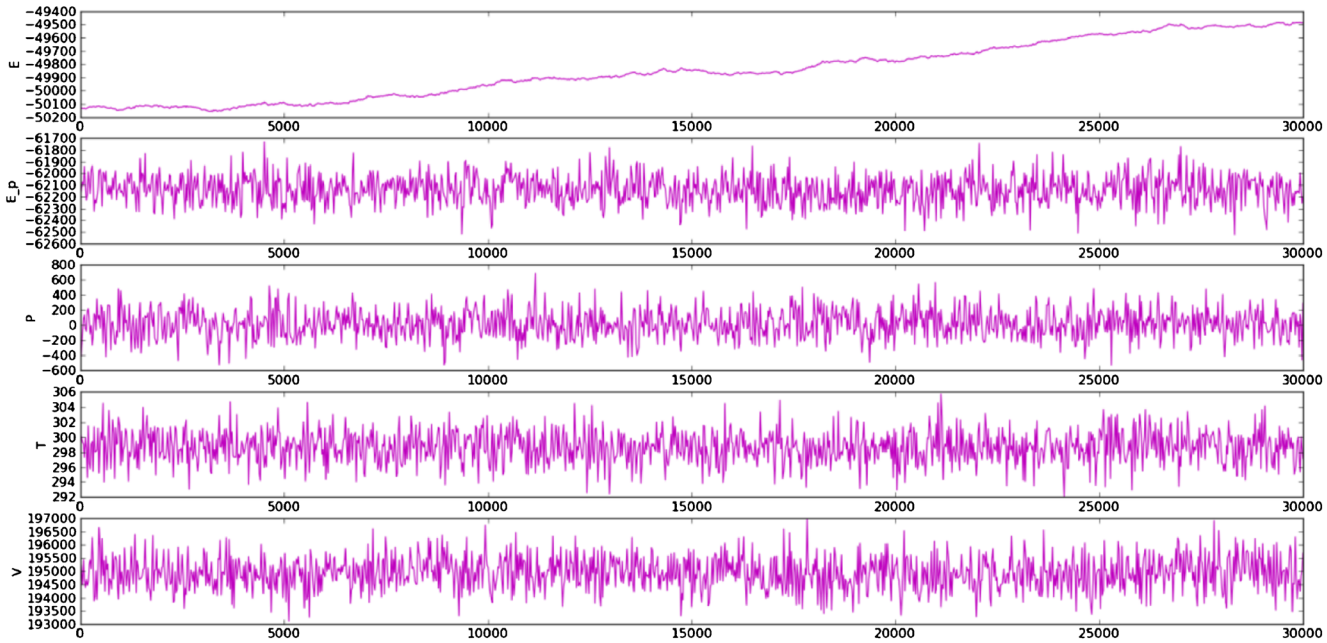

Fig. 4 Energy components of the Cholera toxin- Methyl-α-9-*N*-benzoyl-amino-9-deoxy-Neu5Ac (BENZ) complex during 30 ns molecular dynamic simulation run

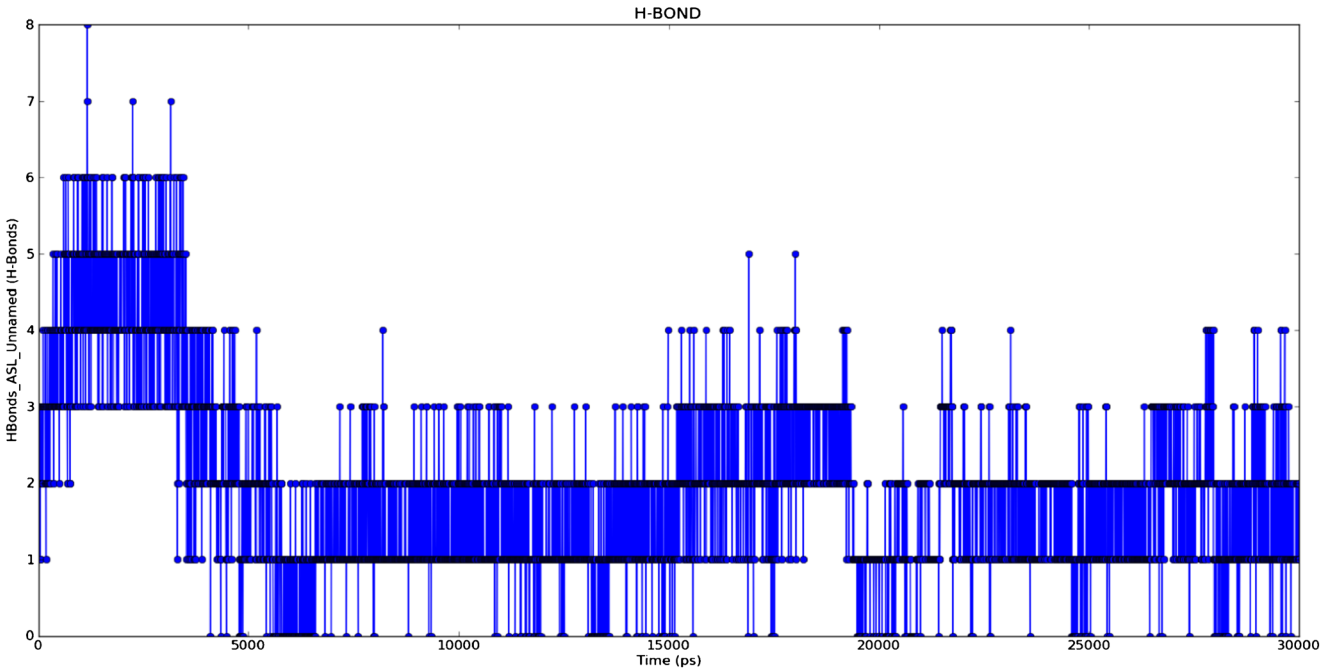

Fig. 5 Hydrogen bond formed between Cholera toxin- Methyl-α-9-*N*-benzoyl-amino-9-deoxy-Neu5Ac (BENZ) complex during 30,000 ps MD simulation run

omega (ω) angle preferred to be trans conformation. The phi ( ) angle for ALA:97 transition occurred between the range of −130° to −80°, for psi (ψ) angle transition was between the range of 10° to 30° and omega (ω) angle preferred to be trans conformation. The phi ( ) angle for ILE:99 transition occurred between the range of −150° to −100° and phi ( ) angle for TYR:12 transition occurred between the range of −140° to −70°. Where psi (ψ) angle and omega (ω) angle for ILE:99 and TYR:12 residues prefer to be trans conformation of 180°.

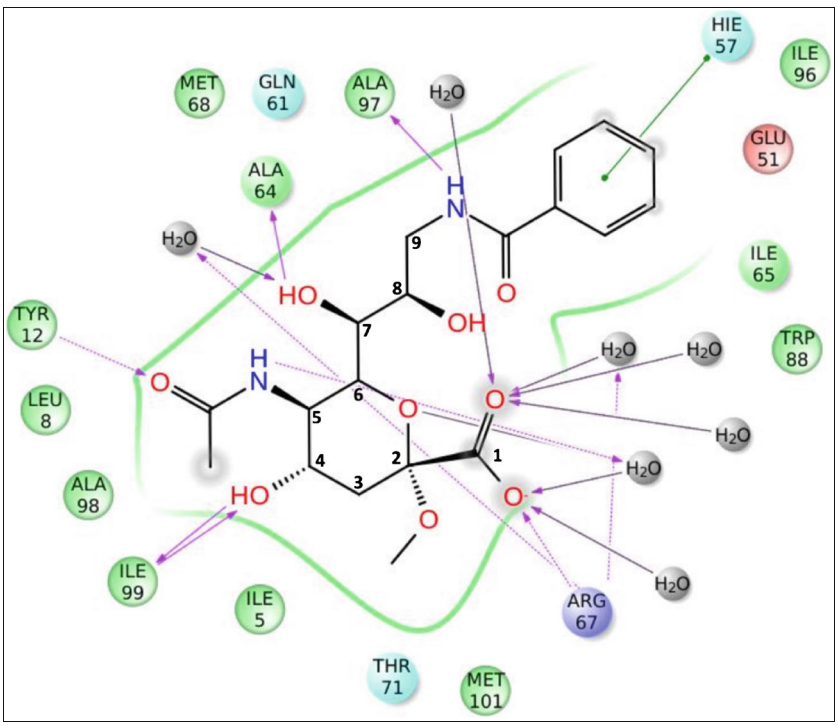

Fig. 6 Intermolecular H-bond interaction of Cholera toxin-Methyl-α-9-*N*-benzoyl-amino-9-deoxy-Neu5Ac (BENZ) complex after 30 ns MD simulation run (Note: ····· H-bond (side chain), ——— H-bond (backbone), ●—● π-π stacking)

Table 4 Inter molecular hydrogen bond distance between Cholera toxin- Methyl-α-9-N-benzoyl-amino-9-deoxy-Neu5Ac (BENZ) complex for 30 ns, CT- Methyl-α-9-N-acetyl-9-deoxy-9-amino-Neu5Ac complex for 10 ns and CT- Methyl-α-9-N-biphenyl-4-acetyl-deoxy-amino-Neu5Ac for 10 ns simulation run

Methyl-α-Neu5Ac analogues	MD simulation (ns)	Total NO. of interaction	Protein		Ligand atoms	Distance Å
			Residues	Atoms		
Methyl-α-9-*N*-benzoyl-amino-9-deoxy-Neu5Ac (BENZ)	30 ns	6	ALA:97	O	H49	2.104
			TYR:12	HH	O	2.210
			ILE:99	H	O	1.938
			ILE:99	O	H35	1.962
			ALA:64	O	H48	2.374
			ARG:67	HH12	O55	1.815
Methyl-α-9-*N*-acetyl-9-deoxy-9-amino-Neu5Ac	10 ns	4	ASN:14	HD21	O	1.928
			LYS:91	HZ1	O48	1.601
			GLN:61	HE22	O	2.222
			TRP:88	HE1	O	1.729
Methyl-α-9-*N*-biphenyl-4-acetyl-deoxy-amino-Neu5Ac	10 ns	5	TRP:88	HE1	O	1.894
			HIS:13	H	O	1.853
			ASN:90	HD22	O	1.765
			HIS:57	HE2	O	2.061
			GLN:61	HE22	O	1.671

MD simulation for CT-Methyl-α-9-*N*-acetyl-9-deoxy-9-amino-Neu5Ac complex

The hydrogen bond interaction for CT-Methyl-α-9-*N*-acetyl-9-deoxy-9-amino-Neu5Ac complex was calculated for the trajectory 10,000 ps obtained after MD simulation. Inter molecular hydrogen bonding was reproduced in MD simulation trajectory data for the complex CT-Methyl-α-9-*N*-acetyl-9-deoxy-9-amino-Neu5Ac. The atom (O) of Methyl-α-9-*N*-acetyl-9-deoxy-9-amino-Neu5Ac formed H-bond with atom (H) HD21 of ASN:14 with a H-bond distance of 1.928 Å, atom 48 (O) of Methyl-α-9-*N*-acetyl-9-deoxy-9-amino-Neu5Ac formed H-bond with atom (H) HZ1 of LYS:91 with a distance of 1.601 Å, atom (O) of Methyl-α-9-*N*-acetyl-9-deoxy-9-amino-Neu5Ac formed H-bond with atom (H) HE22 of GLN:61 with a distance of 2.222 Å & atom (O) of Methyl-α-9-*N*-acetyl-9-deoxy-9-amino-Neu5Ac formed H-bond with atom (H) HE1 of TRP:88 with a distance of 1.729 Å. During MD simulation, the above four hydrogen bonds show stable interaction towards the active site of CT (Fig. 9). In addition to that, water bridging H-bond was formed as CT, GLN:61- H_2O- (O) of Methyl-α-9-*N*-acetyl-9-deoxy-9-amino-Neu5Ac. The analogue Methyl-α-9-*N*-acetyl-9-deoxy-9-amino-Neu5Ac blocks ASN:14, LYS:91, GLN:61 and TRP:88 residues of CT through inter molecular hydrogen bonding. The previous NMR spectroscopy study reported that, the sialic acid inhibits the active site residues of rhesus rotavirus hemagglutinin which is responsible for host specificity [43].

The conformational change occurred during MD simulation (Fig. 10) was calculated for the active site residues of CT, ASN:14, LYS:91, GLN:61 and TRP:88. The phi ( ) angle of

Table 5 Inter molecular hydrogen bond through water bridges, Cholera toxin- Methyl-α-9-N-benzoyl-amino-9-deoxy-Neu5Ac (BENZ) complex for 30 ns, CT- Methyl-α-9-N-acetyl-9-deoxy-9-amino-Neu5Ac complex for 10 ns and CT- Methyl-α-9-*N*-biphenyl-4-acetyl-deoxy-amino-Neu5Ac for 10 ns simulation run

Methyl-α-Neu5Ac analogues	MD simulation (ns)	Total NO. of interaction	Protein		Bridging water	Distance Å	Ligand atoms	Distance Å
			Residues	Atoms				
Methyl-α-9-*N*-benzoyl-amino-9-deoxy-Neu5Ac (BENZ)	30 ns	2	ARG:67	HH11	H_2O	1.637	H48	2.991
			ARG:67	HH22	H_2O	2.090	O	3.148
Methyl-α-9-*N*-acetyl-9-deoxy-9-amino-Neu5Ac	10 ns	1	GLN:61	HE22	H_2O	3.453	O	1.958
Methyl-α-9-*N*-biphenyl-4-acetyl-deoxy-amino-Neu5Ac	10 ns	1	ASN:90	HD21	H_2O	1.935	O	2.651

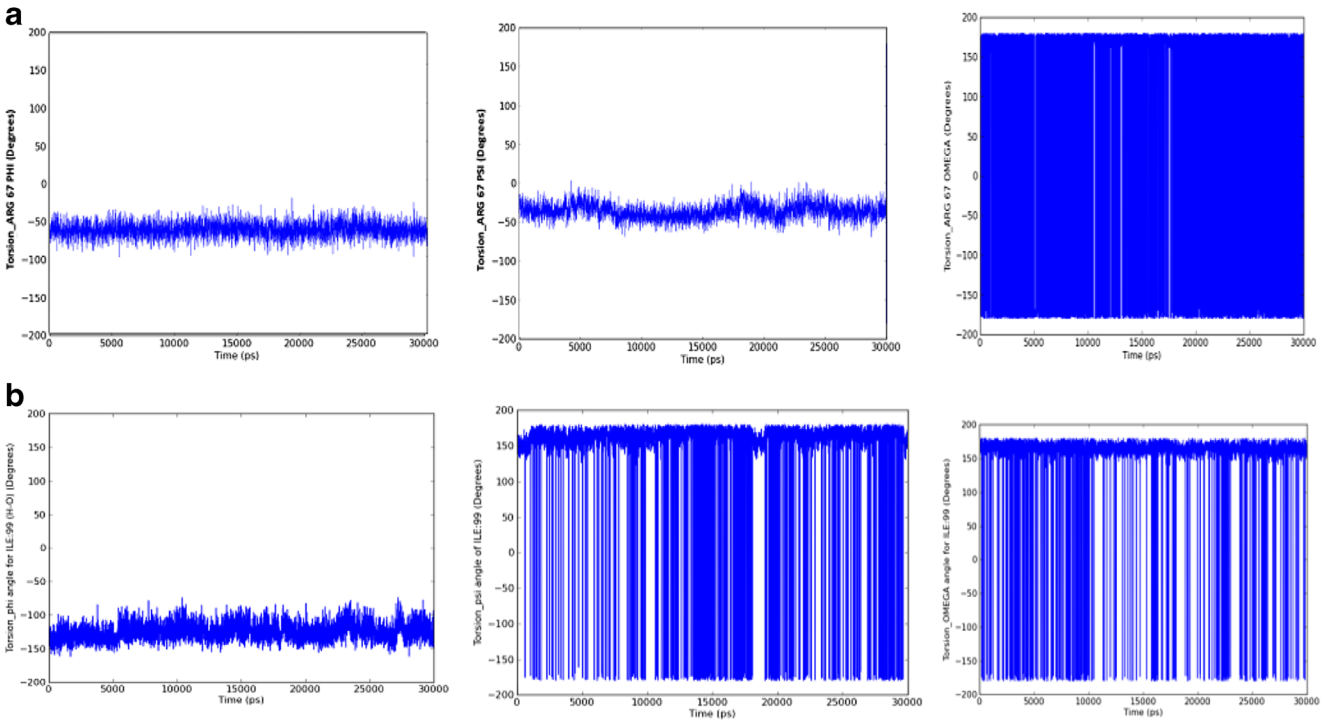

Fig. 7 The conformational plot of Phi ( ), Psi (ψ) and Omega (ω) for the amino acid residues (A) ARG:67 and (B) ILE:99 of Cholera toxin- Methyl-α-9-*N*-benzoyl-amino-9-deoxy-Neu5Ac (BENZ) complex during 30 ns molecular dynamic simulation

ASN:14 shows a transition between the range of 30° to 90°, for psi (ψ) angle transition occurred between the range of −40° to 40° and omega (ω) angle preferred to be trans conformation of 180°. The phi (φ) angle of LYS:91 prefers in some trajectory to be in trans conformation, but majority of the trajectory transition occurred between the range −170° to −90°. Psi (ψ) angles in some of the trajectory are in trans conformation, however majority of the trajectory transition occurred between the range of 130° to 180° and omega (ω) angle preferred to be trans conformation of 180°. For GLN:61, phi (φ) angle transition occurred between the range of 100° to 40°, for psi (ψ) angle transition occurred

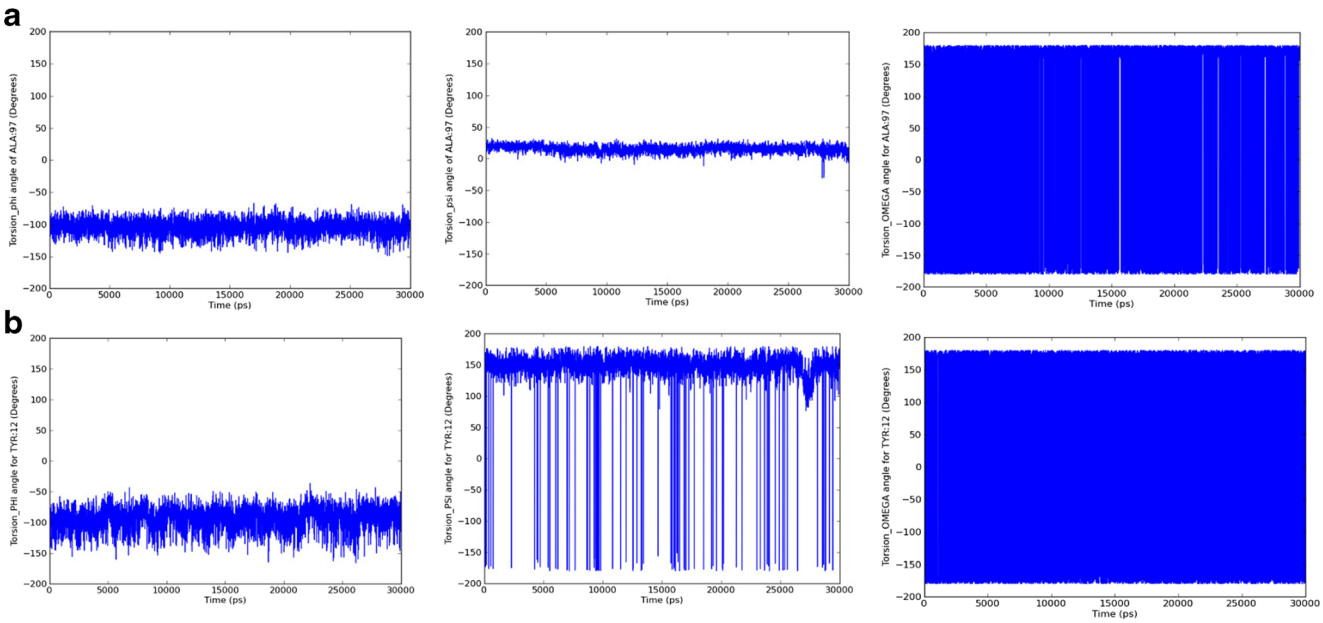

Fig. 8 The conformational plot of Phi ( ), Psi (ψ) and Omega (ω) for the amino acid residues (**a**) ALA:97 and (**b**) TYR:12 of Cholera toxin- Methyl-α-9-*N*-benzoyl-amino-9-deoxy-Neu5Ac (BENZ) complex during 30 ns molecular dynamic simulation run

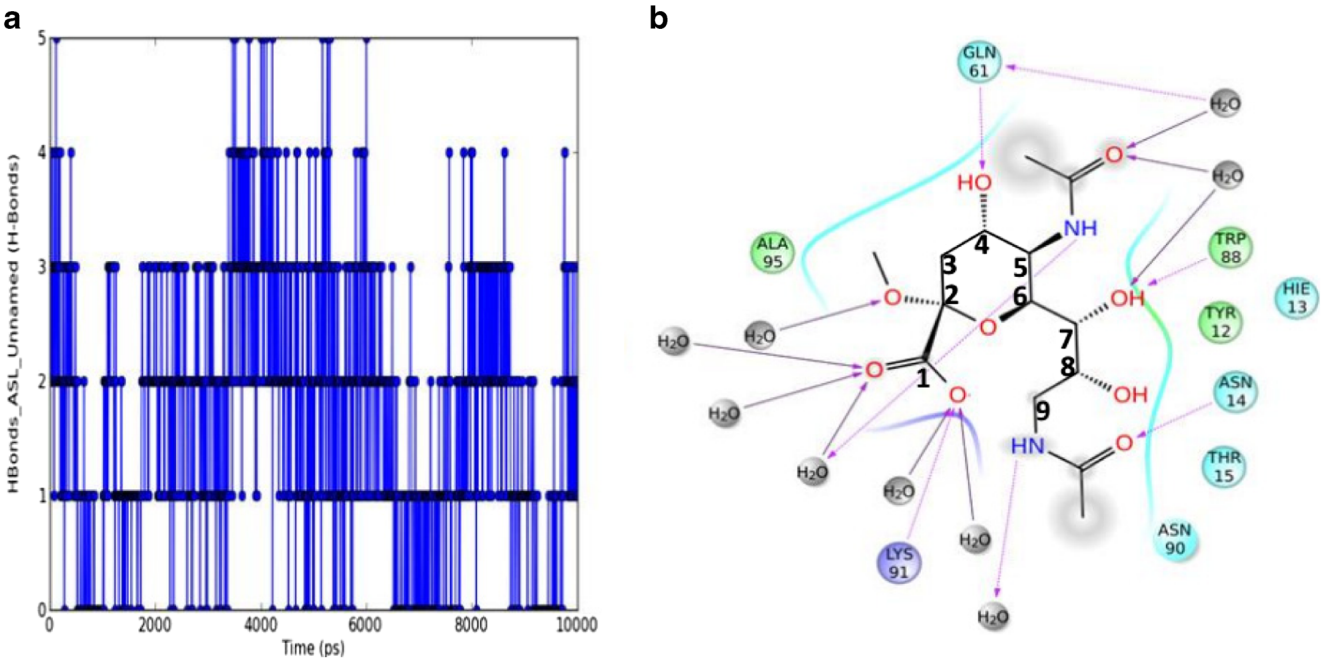

Figure 9 (**a**) Hydrogen bond pattern and (**b**) Intermolecular H-bond interaction between CT- Methyl-α-9-*N*-acetyl-9-deoxy-9-amino-Neu5Ac complex for 10 ns simulation run (Note:⋯⋯ H-bond (side chain), ——— H-bond (backbone))

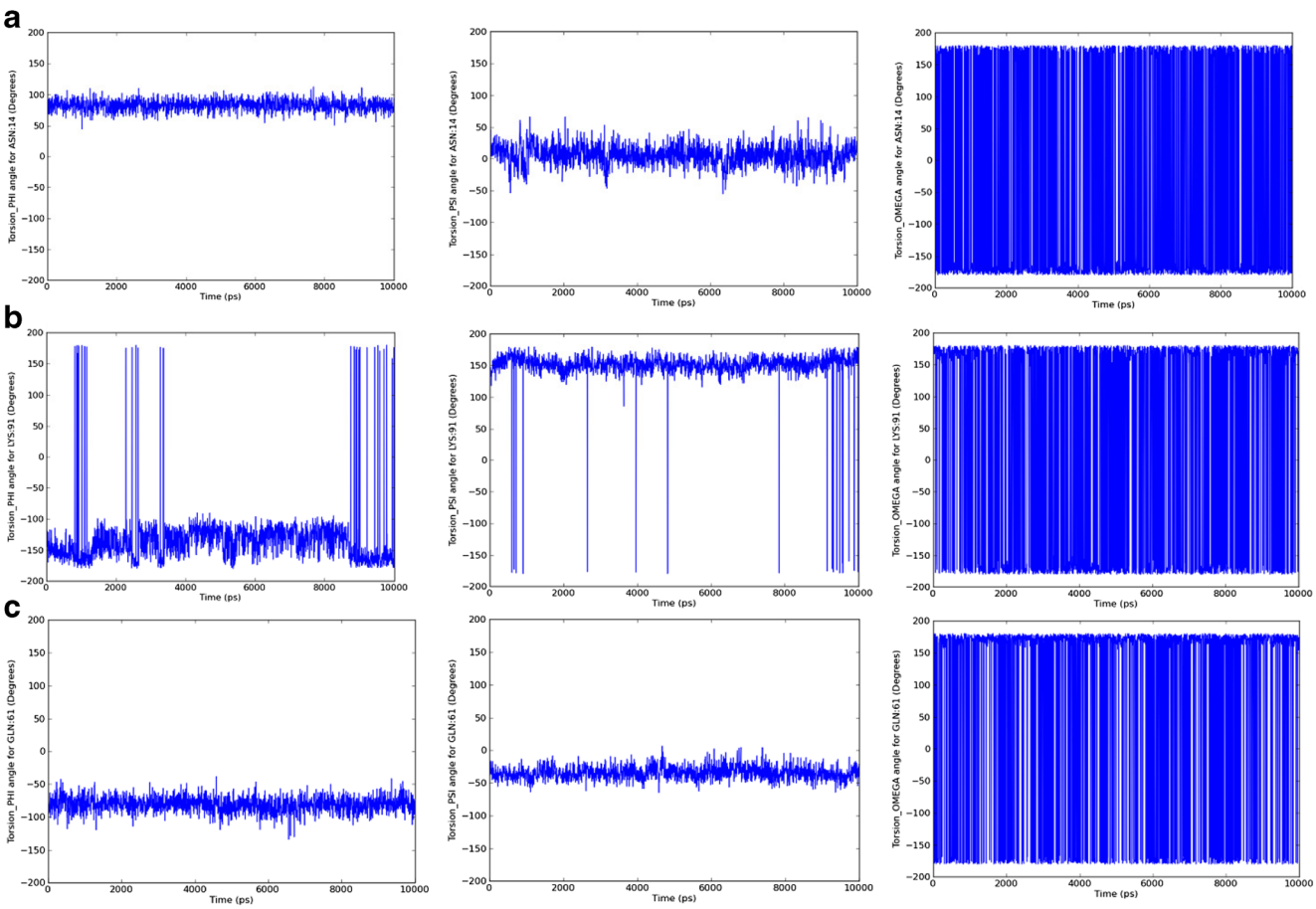

Figure 10 The conformation plot for Phi (φ), Psi (ψ) and Omega (ω) angle for the residues (**a**) ASN:14, (**b**) LYS:91 and (**c**) GLN:61of CT- Methyl-α-9-*N*-acetyl-9-deoxy-9-amino-Neu5Ac complex for 10 ns simulation run

between the range of −50° to -10° and omega (ω) angle preferred to be trans conformation of 180°. The phi (φ) angle of TRP:88 shows a transition between the range of 80° to 120°, for psi (ψ) angle transition occurred between the range of 100° to 150° and omega (ω) angle preferred to be trans conformation of 180°.

MD simulation for CT- Methyl-α-9-*N*-biphenyl-4-acetyl-deoxy-amino-Neu5Ac complex

The hydrogen bond interaction for CT- Methyl-α-9-*N*-biphenyl-4-acetyl-deoxy-amino-Neu5Ac complex was calculated for 10,000 ps simulation run (Fig. 11). The atom (O) of Methyl-α-9-*N*-biphenyl-4-acetyl-deoxy-amino-Neu5Ac formed H-bond with atom (H) HE1 of TRP:88 with a distance of 1.894 Å, atom (O) of Methyl-α-9-*N*-biphenyl-4-acetyl-deoxy-amino-Neu5Ac formed H-bond with atom (H) of HIS:13 with a distance of 1.853 Å, atom (O) of Methyl-α-9-*N*-biphenyl-4-acetyl-deoxy-amino-Neu5Ac formed H-bond with atom (H) HD22 of ASN:90 with a distance of 1.765 Å, atom (O) of Methyl-α-9-*N*-biphenyl-4-acetyl-deoxy-amino-Neu5Ac formed H-bond with atom (H) HE2 of HIS:57 with a distance of 2.061 Å, atom (O) of Methyl-α-9-*N*-biphenyl-4-acetyl-deoxy-amino-Neu5Ac formed H-bond with atom (H) HE22 of GLN:61 with a distance of 1.671 Å. In addition to that, a water mediating H-bond was formed as CT, ASN:90 - H_2O - (O) of Methyl-α-9-*N*-biphenyl-4-acetyl-deoxy-amino-Neu5Ac.

The dihedral angle phi (φ), psi (ψ) and omega (ω) angle were calculated for the active site residues TRP:88, HIS:13, ASN:90, HIS:57 & GLN:61 which formed stable H-bond interaction after MD simulation (Fig. 12). Similar binding site residues were suggested by earlier saturation transfer difference (STD) NMR study for influenza hemagglutinin as TRP:156, HIS:183 and HIS:186 [44]. The phi (φ) angle of TRP:88 shows a transition between the range of −110° to −50°, for psi (ψ) angle transition occurred between the range of 100° to 150° and omega (ω) angle preferred to be trans conformation of 180°. The phi (φ) angle of HIS:13 shows a transition between the range of −130° to −70°, for psi (ψ) angle transition occurred between the range of 110° to 160° and omega (ω) angle preferred to be trans conformation of 180°. The phi (φ) angle of ASN:90 shows a transition between the range of −150° to −60°, for psi (ψ) angle transition occurred between the range of −30° to 50° and omega (ω) angle preferred to be trans conformation of 180°. The phi (φ) angle of HIS:57 shows a transition between the range of −120° to −30°, for psi (ψ) angle transition occurred between the range of 130° to 180°, but in some trajectories it was in trans conformation and omega (ω) angle preferred to be trans conformation of 180°. The phi (φ) angle of GLN:61 shows a transition between the range of −100° to −50°, for psi (ψ) angle transition occurred between the range of −60° to −30° and omega (ω) angle preferred to be trans conformation of 180°.

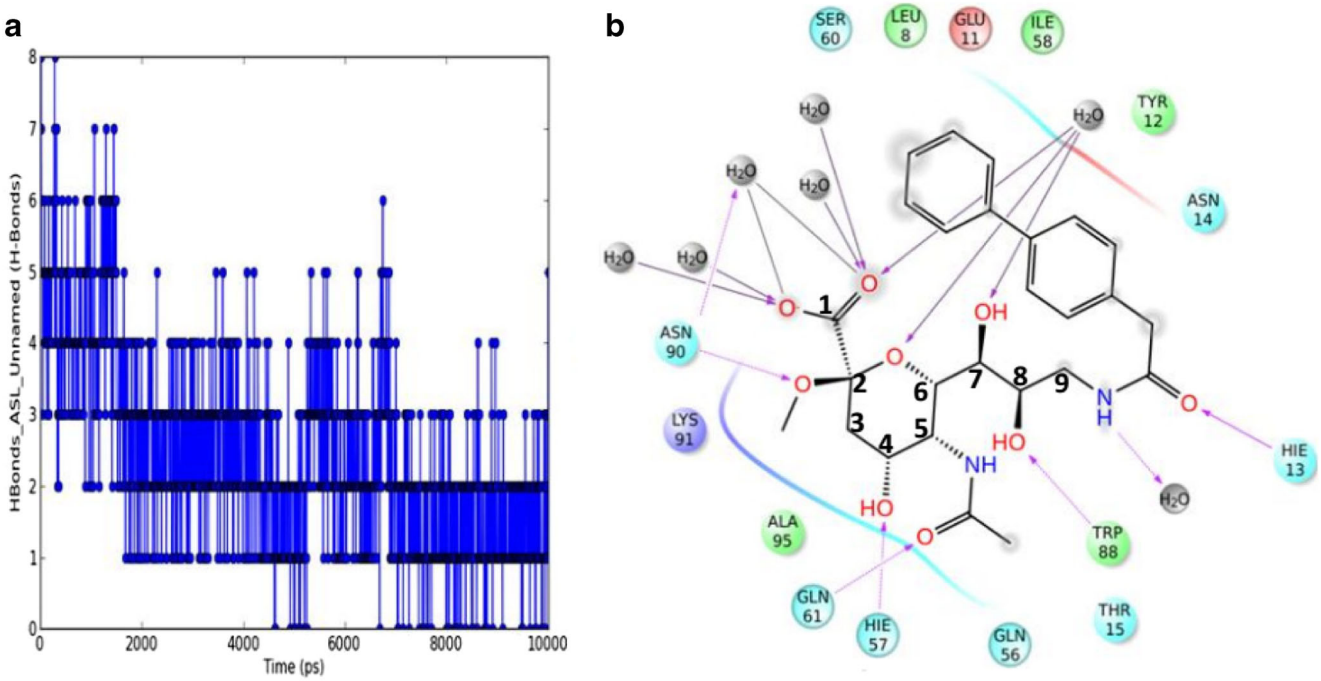

Figure 11 (**a**) Hydrogen bond pattern and (**b**) Intermolecular H-bond interaction between CT- Methyl-α-9-*N*-biphenyl-4-acetyl-deoxy-amino-Neu5Ac complex for 10 ns simulation run (Note: ····· H-bond (side chain), ——— H-bond (backbone))

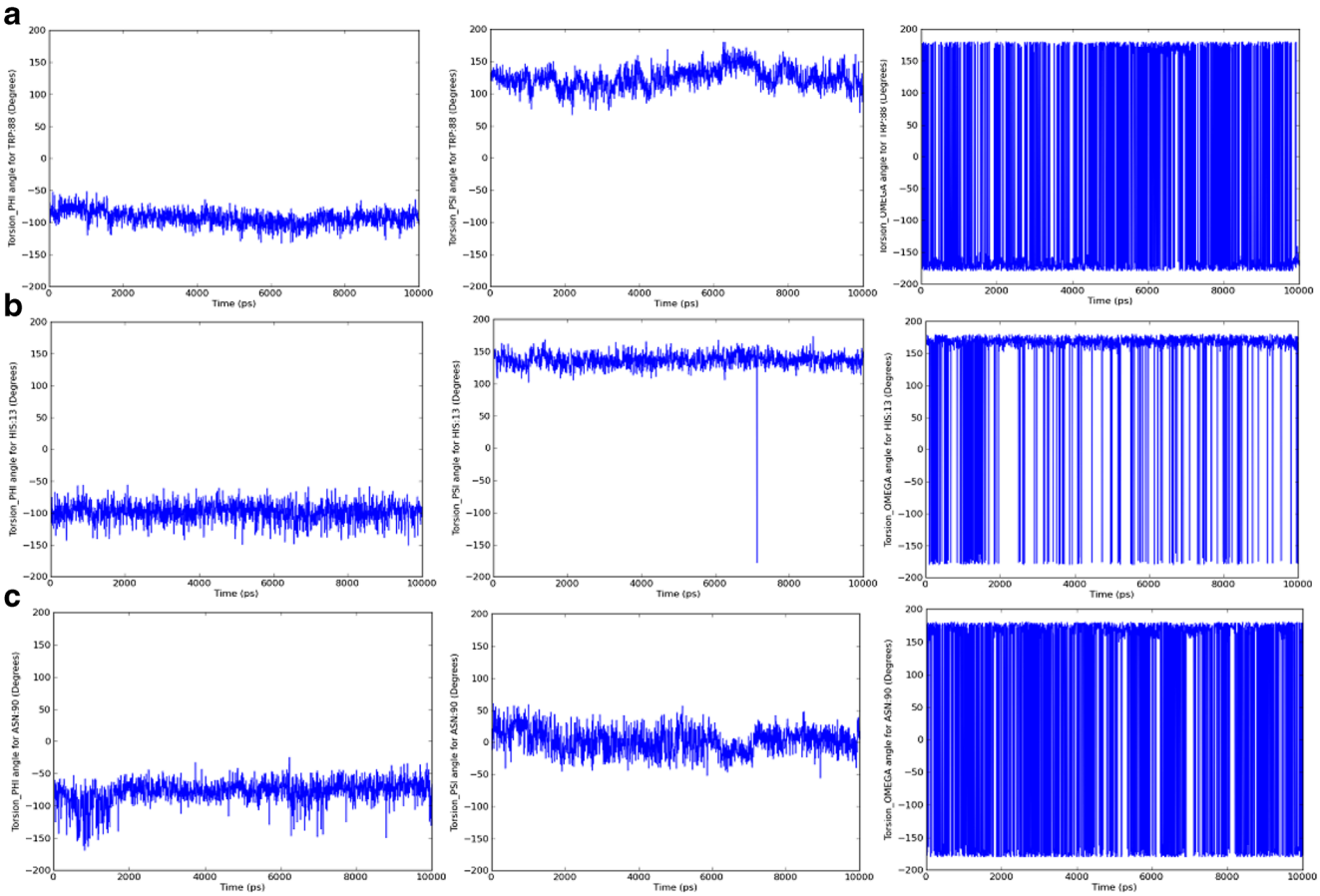

Fig. 12 The conformation plot for Phi (φ), Psi (ψ) and Omega (ω) angle for the residues (A) TRP:88, (B) HIS:13 and (C) ASN:90 of CT- Methyl-α-9-*N*-biphenyl-4-acetyl-deoxy-amino-Neu5Ac complex for 10 ns simulation run

Glycerol side chain conformation of C-9 substituted methyl-α-Neu5Ac analogues

The dynamic behavior of dihedral angles χ_1 and χ_2 (Fig. 13) was calculated for the three analogues: Methyl-α-9-*N*-benzoyl-amino-9-deoxy-Neu5Ac (BENZ), Methyl-α-9-*N*-acetyl-9-deoxy-9-amino-Neu5Ac and Methyl-α-9-*N*-biphenyl-4-acetyl-deoxy-amino-Neu5Ac binding into the active site of CT. For Methyl-α-9-*N*-benzoyl-amino-9-deoxy-Neu5Ac (BENZ), χ_1 prefers −80° to -50° and χ_2 prefers +180° to -180°. Methyl-α-9-*N*-acetyl-9-deoxy-9-amino-Neu5Ac, χ_1 prefers +180° to -180° and χ_2 prefers −70° to −40° till 2200 ps and +40° to +80° from 2200 to 10,000 ps. In Methyl-α-9-*N*-biphenyl-4-acetyl-deoxy-amino-Neu5Ac, χ_1 prefers −30° to −20° and χ_2 prefers trans conformation. An earlier report, sialic acid analogues at C-9 substituted side chain conformation reveals that for the analogues benzyl 2α-*O*-methyl-5-*N*-acetyl-8,9-O-isopropylidene neuraminate, benzyl 2α-*O*-methyl-4-*O*-capriloyl-5-*N*-acetyl-8,9-*O*-isopropylidene neuraminate and benzyl-2α-*O*-methyl-4-*O*-(8-morpholin)-capriloyl-5-*N*-acetyl-8,9-*O*-isopropylidene neuraminate, χ_1 angle prefers to be in trans conformation of +180° to -180° regions and χ_2 angle prefers -70° region [45].

Hydrophobic interaction

Hydrophobic interactions for CT- Methyl-α-Neu5Ac analogue complexes were calculated using the tool Protein-Ligand Attractions Investigations (PLATINUM) [46]. Using this software hydrophobic/hydrophilic property of the two interacting molecules can be calculated. Hydrophobic interactions play a vital role in biomolecular recognition. Methyl-α-9-N-biphenyl-4-acetyl-deoxy-amino-Neu5Ac showed highest hydrophobic value ($S_{L/L}$) of 30.06, followed by Methyl-α-9-N-benzoyl-amino-9-deoxy-Neu5Ac (BENZ) whose hydrophobic value is 7.15 and Methyl-α-9-N-acetyl-9-deoxy-9-amino-Neu5Ac with hydrophobic value of 2.85 (Table 6 and Fig. 14).

The modeled Methyl-α-Neu5Ac analogues were docked against cholera toxin B subunit protein to analyze the interaction and the binding mode of the complex (Table 2) using Glide [18]. All the Methyl-α-Neu5Ac analogues have better pharmacological properties suggesting that the analogues may be considered as suitable candidates for further drug design for cholera disease. Molecular dynamic simulation was done to check the stability of the CT- Methyl-α-Neu5Ac

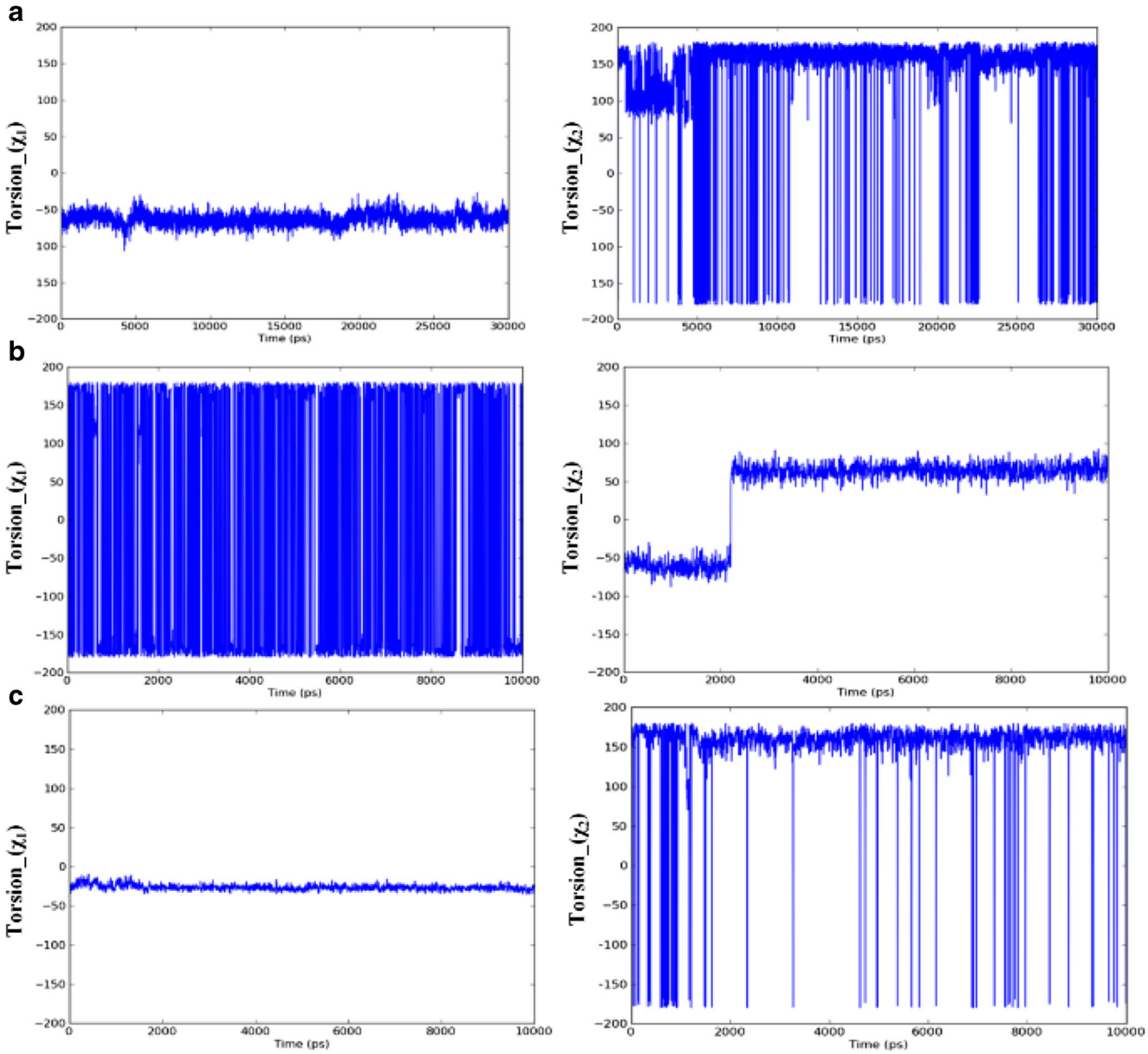

Fig. 13 MD simulation trajectory and χ_1 and χ_2 torsion distribution plot for the analogues (**a**) Methyl-α-9-*N*-benzoyl-amino-9-deoxy-Neu5Ac (BENZ) for 30 ns, (**b**) Methyl-α-9-*N*-acetyl-9-deoxy-9-amino-Neu5Ac for 10 ns and (**c**) Methyl-α-9-*N*-biphenyl-4-acetyl-deoxy-amino-Neu5Ac 10 ns

analogues complex in different time scale using Desmond program [20]. MD simulation was carried out for CT- Methyl-α-9-*N*-benzoyl-amino-9-deoxy-Neu5Ac (BENZ) complex for 30 ns, CT- Methyl-α-9-*N*-acetyl-9-deoxy-9-amino-Neu5Ac complex for 10 ns and CT- Methyl-α-9-*N*-biphenyl-4-acetyl-deoxy-amino-Neu5Ac complex 10 ns. Simulation quality analysis (Energy plot), simulation event analysis (RMSD, RMSF,

Table 6 Hydrophobic/hydrophilic interaction of simulated methyl-α-Neu5Ac analogues

Ligand name	$S_{L/L\ [Hydrophobicity]}$	$S_{H/H\ [Hydrophilicity]}$	S_{buried}	S_{total}	Match[1]	Match[2]
Methyl-α-9-*N*-biphenyl-4-acetyl-deoxy-amino-Neu5Ac	30.06	100.12	244.36	424.61	0.3066	0.2197
Methyl-α-9-*N*-acetyl-9-deoxy-9-amino-Neu5Ac	2.85	105.82	190.12	300.50	0.3616	0.0542
Methyl-α-9-*N*-benzoyl-amino-9-deoxy-Neu5Ac (BENZ)	7.15	97.78	207.15	352.66	0.2975	0.0747
Methyl-α-Neu5Ac	24.37	66.39	209.24	269.30	0.337	0.2801

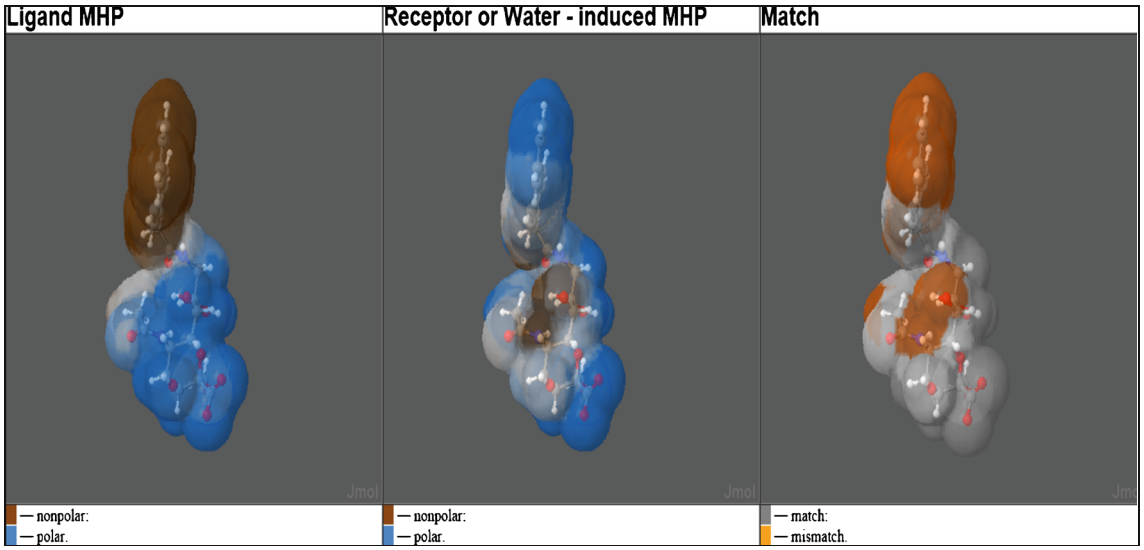

Fig. 14 The hydrophobic/hydrophilic properties of Methyl-α-9-N-biphenyl-4-acetyl-deoxy-amino-Neu5Ac (*left*) and its binding site (*middle*) projected onto the surface of the analogue and their match (*right*). Brown colour indicates hydrophobic region and the blue colour indicates hydrophilic region

Hydrogen bond analysis and Conformational analysis) explains the steady nature of the complex in different time scale. For CT- Methyl-α-9-N-benzoyl-amino-9-deoxy-Neu5Ac (BENZ) complex, the active site residues ARG:67, ILE:99, ALA:97 and TYR:12 forms direct H-bonds and ARG:67 forms two water bridges with Methyl-α-9-N-benzoyl-amino-9-deoxy-Neu5Ac (BENS) (Fig. 6 and Table 5). In C-9 position, due to the presence of aromatic ring the π-π stacking is formed between the aromatic ring at C-9 position of Methyl-α-9-N-benzoyl-amino-9-deoxy-Neu5Ac (BENZ) - CT complex. CT- Methyl-α-9-N-acetyl-9-deoxy-9-amino-Neu5Ac complex binding site residues ASN:14, LYS:91, GLN:61 and TRP:88 produced direct H-bonds and one water mediating H-bond as GLN:61- H_2O - (O) of Methyl-α-9-N-acetyl-9-deoxy-9-amino-Neu5Ac. In a previous report about Lectin-Disaccharides interaction, the residue GLN-53 of lectin formed a water bridge with disaccharides [47]. For CT- Methyl-α-9-N-biphenyl-4-acetyl-deoxy-amino-Neu5Ac complex the amino acid residues TRP:88, HIS:13, ASN:90, HIS:57 & GLN:61 formed direct H-bonds and water bridge as ASN:90 - H_2O - (O) of Methyl-α-9-N-biphenyl-4-acetyl-deoxy-amino-Neu5Ac. The conformational analysis for the protein back bone (phi (, psi (ψ) and omega (ω) angle) and glycerol side chain (χ_1 and χ_2) were calculated to check the stability of the complex. The Methyl-α-Neu5Ac analogues shows better pharmacological properties, binding interaction and conformational stability towards the cholera toxin protein thus Methyl-α-Neu5Ac analogues may be used for designing drug molecule for cholera.

Conclusion

Molecular docking studies reveal that the Methyl-α-Neu5Ac analogues modified in the C-9 position shows better interaction towards the binding site of cholera toxin protein. In the present study, seven Neu5Ac analogues were modeled and docked against cholera toxin B subunit protein. Among the seven Methyl-α-Neu5Ac analogues, Methyl-α-9-*N*-benzoyl-amino-9-deoxy-Neu5Ac (BENZ), Methyl-α-9-*N*-acetyl-9-deoxy-9-amino-Neu5Ac and Methyl-α-9-*N*-biphenyl-4-acetyl-deoxy-amino-Neu5Ac shows least docking (XPG) score and glide energy of −7.55 & −41.48 Kcal/mol, −7.13 & −41.37 Kcal/mol and −6.74 & −48.75 Kcal/mol respectively. Methyl-α-9-*N*-benzoyl-amino-9-deoxy-Neu5Ac (BENZ), Methyl-α-9-*N*-acetyl-9-deoxy-9-amino-Neu5Ac and Methyl-α-9-*N*-biphenyl-4-acetyl-deoxy-amino-Neu5Ac blocks the cholera toxin active site residues through intermolecular hydrogen bonding. MD simulation was done for the complex CT- Methyl-α-9-*N*-benzoyl-amino-9-deoxy-Neu5Ac (BENZ) for 30 ns, CT- Methyl-α-9-*N*-acetyl-9-deoxy-9-amino-Neu5Ac for 10 ns and CT- Methyl-α-9-N-biphenyl-4-acetyl-deoxy-amino-Neu5Ac for 10 ns. The RMSD, RMSF and Energy plot explain that the complex was stable throughout the simulation trajectories. For the complex CT-Methyl-α-9-*N*-benzoyl-amino-9-deoxy-Neu5Ac (BENZ) the residues ALA:97, ILE:99, TYR:12, ARG:67 and ALA:64 show stable H-bond interaction during 30 ns simulations run and two additional water bridges were generated in some trajectories by active site residue ARG:67. For the complex CT- Methyl-α-9-*N*-acetyl-9-deoxy-9-amino-Neu5Ac, the active site residues ASN:14, LYS:91, GLN:61 and TRP:88 maintain the constant H-bond interaction and one additional

water bridge was formed by the residue GLN:61 for 10 ns & for the complex CT- Methyl-α-9-*N*-biphenyl-4-acetyl-deoxy-amino-Neu5Ac, the active site residuesTRP:88, HIS:13, ASN:90, HIS:57 and GLN:61 shows constant H-bond interaction and one water bridge was produced by the residue ASN:90 for 10 ns simulation time. The MD trajectory data discloses the binding orientations of three Methyl-α-Neu5Ac analogues that favorably fits in the binding pocket of cholera toxin and shows acceptable pharmacological properties. Therefore Methyl-α-9-*N*-benzoyl-amino-9-deoxy-Neu5Ac (BENZ), Methyl-α-9-*N*-acetyl-9-deoxy-9-amino-Neu5Ac and Methyl-α-9-*N*-biphenyl-4-acetyl-deoxy-amino-Neu5Ac may be considered for designing drug molecules against cholera disease.

Acknowledgments The authors acknowledge the financial support given by SERB (Science and Engineering Research Board, DST) Ref No. (SR/FT/LS-157/2009), Govt. of India, New Delhi.

References

1. Corfield, A. P., Schauer, R., in Schauer, R. (Ed.), Sialic acids: chemistry, metabolism and function. Cell Biology Monographs. **10** 195–261. Springer Wien, Vienna (1982)
2. Simanek, E.E., McGarvey, G.J., Jablonowski, J.A., Wong, C.-H.: Selectin-Carbohydrate Interactions: from natural ligands to designed mimics. Chem. Rev. **98**, 833–862 (1998)
3. Kiefel, M.J., von Itzstein, M.: Recent advances in the synthesis of sialic acid derivatives and sialylmimetics as biological probes. Chem. Rev. **102**, 471–490 (2002)
4. Royle, L., Matthews, E., Corfield, A., Berry, M., Rudd, P.M., Dwek, R.A., Carrington, S.D.: Glycan structures of ocular surface mucins in man, rabbit and dog display species differences. Glycoconj. J. **25**, 763–773 (2008)
5. Varki, A.: Sialic acids in human health and disease. Trends Mol. Med. **14**, 351–360 (2008)
6. Woronowicz, A., Amith, S.R., De Vusser, K., Laroy, W., Contreras, R., Basta, S., Szewczuk, M.R.: Dependence of neurotrophic factor activation of Trk tyrosine kinase receptors on cellular sialidase. Glycobiology **17**, 10–24 (2006)
7. Schauer, R.: in Sansom, C., Markman O. (Eds.), The diversity of sialic acids and their interplay with lectins. Glycobiology. Scion Bloxham, 136–149 (2007)
8. Zaccai, N.R., Maenaka, K., Maenaka, T., Crocker, P.R., Brossmer, R., Kelm, S., Jones, E.Y.: Structure-guided design of sialic acid-based siglec inhibitors and crystallographic analysis in complex with sialoadhesin. Structure **11**, 557–567 (2003)
9. Lehmann, F., Tiralongo, E., Tiralongo, J.: Sialic acid-specific lectins: occurrence, specificity and function. Cell. Mol. Life Sci. **63**, 1331–1354 (2006)
10. Heyningen, W.E.V.: Membrane receptors for bacterial toxins. Surface Membrane Receptors. 147–167 (1976)
11. Sharmila, D.J.S., Veluraja, K.: Monosialogangliosides and Their Interaction with cholera toxin – investigation by molecular modeling and molecular mechanics. J. Biomol. Struct. Dyn. **21**, 591–613 (2004)
12. Sharmila, D.J.S., Veluraja, K.: Disialogangliosides and their interaction with cholera toxin – investigation by molecular modeling, molecular mechanics and molecular dynamics. Journal of Biomolecular Structure & Dynamics. **22**, 299–313 (2004)
13. Sharmila, D.J.S., Veluraja, K.: Conformations of higher gangliosides and their binding with cholera toxin – investigation by molecular modeling, molecular mechanics, and molecular dynamics. J. Biomol. Struct. Dyn. **23**, 641–656 (2006)
14. Branson, T.R., Turnbull, W.B.: Bacterial toxin inhibitors based on multivalent scaffolds. Chem. Soc. Rev. **42**, 4613 (2013)
15. Branson, T.R., McAllister, T.E., Garcia-Hartjes, J., Fascione, M.A., Ross, J.F., Warriner, S.L., Wennekes, T., Zuilhof, H., Turnbull, W.B.: A protein-based pentavalent inhibitor of the cholera toxin B-subunit. Angew. Chem. Int. Ed. **53**, 8323–8327 (2014)
16. Merritt, E.A., Kuhn, P., Sarfaty, S., Erbe, J.L., Holmes, R.K., Hol, W.G.J.: The 1.25 Å resolution refinement of the cholera toxin B-pentamer: evidence of peptide backbone strain at the receptor-binding site. J. Mol. Biol. **282**, 1043–1059 (1998)
17. Lengauer, T., Rarey, M.: Computational methods for biomolecular docking. Curr. Opin. Struct. Biol. **6**, 402–406 (1996)
18. Friesner, R.A., Murphy, R.B., Repasky, M.P., Frye, L.L., Greenwood, J.R., Halgren, T.A., Sanschagrin, P.C., Mainz, D.T.: Extra precision glide: docking and scoring incorporating a model of hydrophobic enclosure for protein-ligand complexes. J. Med. Chem. **49**, 6177–6196 (2006)
19. Alder, B.J., Wainwright, T.E.: Studies in molecular dynamics. I. General Method. J. Chem. Phys. **31**, 459 (1959)
20. Shan, Y., Kim, E.T., Eastwood, M.P., Dror, R.O., Seeliger, M.A., Shaw, D.E.: How does a drug molecule find its target binding site? J. Am. Chem. Soc. **133**, 9181–9183 (2011)
21. Maestro 9.0, versuib 70110, Schrodinger, New York (2009)
22. Kaminski, G.A., Friesner, R.A., Tirado-Rives, J., Jorgensen, W.L.: Evaluation and reparametrization of the OPLS-AA force field for protein via comparison with accurate quantum chemical calculations on peptides. J. Phys. Chem. B **105**, 6474–6487 (2001)
23. Brooks, W.H., Daniel, K.G., Sung, S.S., Guida, W.C.: Computational validation of the importance of absolute stereochemistry in virtual screening. J. Chem. Inf. Model. **48**, 639–645 (2008)
24. Chen, I.J., Foloppe, N.: Drug-like bioactive structures and conformational coverage with the LigPrep/ ConfGen suite: comparison to programs MOE and catalyst. J. Chem. Inf. Model. **50**, 822–839 (2010)
25. Friesner, R.A., Banks, J.L., Murphy, R.B., Halgren, T.A., Klicic, J.J., Mainz, D.T., Repasky, M.P., Knoll, E.H., Shelley, M., Perry, J.K., Shaw, D.E., Francis, P., Shenkin, P.S.: Glide: a new approach for rapid, accurate docking and scoring. 1. Method and assessment of docking accuracy. J. Med. Chem. **47**, 1739–1749 (2004)
26. Jorgensen, W.L., Duffy, E.M.: Prediction of drug solubility from structure. Adv. Drug Deliv. Rev. **54**, 355–366 (2002)
27. QikProp3.2, Schrodinger LLC, New York, NY (2009)
28. Lipinski, C., Hopkins, A.: Navigating chemical space for biology and medicine. Nature **432**, 855–861 (2004)
29. Jorgensen, W.L., Chandrasekhar, J., Madura, J.D., Impey, R.W., Klein, M.L.: Comparison of simple potential functions for simulating liquid water. The Journal of Chemical Physics. **79**, 926 (1983)
30. Strahan, G.D., Keniry, M.A., Shafer, R.H.: NMR structure refinement and dynamics of the K+−[d(G3T4G3)]2 quadruplex via particle mesh Ewald molecular dynamics simulations. Biophys. J. **75**, 968–981 (1998)
31. Essmann, U., Perera, L., Berkowitz, M.L., Darden, T., Lee, H., Pedersen, L.G.: A smooth particle mesh Ewald method. The Journal of Chemical Physics. **103**, 8577 (1995)
32. Andersen, H.C.: Rattle: a "velocity" version of the shake algorithm for molecular dynamics calculations. J. Comput. Phys. **52**, 24–34 (1983)
33. Barb, A.W., Wang, X., Prestegard, J.H.: Refolded recombinant Siglec5 for NMR investigation of complex carbohydrate binding. Protein Expression Purification. **88**, 183–189 (2013)
34. Lipinski, C.A.: Drug-like properties and the causes of poor solubility and poor permeability. Journal of Pharmacological Toxicological Methods. **44**, 235–249 (2000)

35. Lipinski, C.A., Lombardo, F., Dominy, B.W., Feeney, P.J.: Experimental and computational approaches to estimate solubility and permeability in drug discovery and development settings. Adv. Drug Deliv. Rev. **23**, 3–25 (1997)
36. Lugsanangarma, K., Pianwanit, S., Kokpol, S., Tanaka, F.: Homology modelling and molecular dynamic simulations of wild type and mutated flavodoxins from Desulfovibrio vulgaris (Miyazaki F): insight into FMN- apoprotein interactions. Mol. Simul. **37**, 1164–1178 (2011)
37. Chubb, A.J., Fitzgerald, D.J., Nolan, K.B., Moman, E.: The productive conformation of prostaglandin G2 at the peroxidase site of prostaglandin endoperoxide H synthase: docking, molecular dynamics, and site-directed mutagenesis studies. Biochemistry **45**, 811–820 (2006)
38. Hayes, J.M., Skamnaki, V.T., Archontis, G., Lamprakis, C., Sarrou, J., Bischler, N., Skaltsounis, A.-L., Zographos, S.E., Oikonomakos, N.G.: Kinetics, in silico docking, molecular dynamics, and MM-GBSA binding studies on prototype indirubins, KT5720, and staurosporine as phosphorylase kinase ATP-binding site inhibitors: The role of water molecules examined. Proteins: Structure, Function, and Bioinformatics **79**, 703–719 (2011)
39. Li, M.H., Luo, Q., Xue, X.G., Li, Z.S.: Molecular dynamics studies of the 3D structure and planar ligand binding of a quadruplex dimer. J. Mol. Model. **17**, 515–526 (2010)
40. Saraboji, K., Hakansson, M., Genheden, S., Diehl, C., Qvist, J., Weininger, U., Nilsson, U.J., Leffler, H., Ryde, U., Akke, M., Logan, D.T.: The carbohydrate-binding site in galectin-3 is preorganized to recognize a sugarlike framework of oxygens: ultra-high-resolution structures and water dynamics. Biochemistry **51**, 296–306 (2012)
41. Kumar, S., Frank, M., Schwartz-Albiez, R.: Understanding the specificity of human galectin-8C domain interactions with its glycan ligands based on molecular dynamics simulations. PLoS One **8**, e59761 (2013)
42. Song, J., Tan, H., Wang, M., Webb, G.I., Akutus, T.: TANGLE: two-level support vector regression approach for protein backbone torsion angle prediction from primary sequences. PLoS One **7**, e30361 (2012)
43. Dormitzer, P.R., Sun, Z.Y.J., Blixt, O., Paulson, J.C., Wagner, G., Harrison, S.C.: Specificity and affinity of sialic acid binding by the rhesus rotavirus VP8* core. J. Virol. **76**, 10512–10517 (2002)
44. McCullough, C., Wang, M., Rong, L., Caffrey, M.: Characterization of influenza hemagglutinin interactions with receptor by NMR. PLoS One **7**, e33958 (2012)
45. Blessia, T.F., Rapheal, V.S., Sharmila, D.J.S.: Molecular dynamics of sialic acid analogues and their interaction with influenza hemagglutinin. Indian journal of pharmaceutical sciences. **72**, 449–457 (2010)
46. Pyrkov, T.V., Chugunov, A.O., Krylov, N.A., Nolde, D.E., Efremov, R.G.: PLATINUM: a web tool for analysis of hydrophobic/hydrophilic organization of biomolecular complexes. Bioinformatics **25**, 1201–1202 (2009)
47. Nurisso, A., Blanchard, B., Audfray, A., Rydner, L., Oscarson, S., Varrot, A., Imberty, A.: Role of water molecules in structure and energetics of Pseudomonas aeruginosa lectin I interacting with disaccharides. J. Biol. Chem. **285**, 20316–20327 (2010)